

1
2
3
4
5
6
7
8
9
10
11
12
13
14
15
16
17
18
19
20
21
22
23
24
25
26
27
28
29
30
31
32
33
34
35
36
37
38
39
40
41
42
43
44
45
46
47
48
49
50
51
52
53
54
55
56
57
58
59
60
61
62
63
64
65

Global warming of the mantle beneath continents back to the Archean

Nicolas Coltice (1), Hervé Bertrand (1), Patrice Rey (2), Frédéric Jourdan (3), Benjamin R. Philipps (4), Yanick Ricard (1)

1. Laboratoire de Sciences de la Terre, UMR-CNRS 5570, Université de Lyon, Université Claude Bernard Lyon 1, Bat Géode, 2 rue Raphael Dubois, 69622 Villeurbanne Cedex, France

2. School of Geosciences, University of Sydney, Edgeworth Building, NSW2006 Sydney, Australia

3. Western Australian Argon Isotope Facility, Department of Applied Geology & JdL Centre, Curtin university of Technology, GPO Box U1987, Perth, WA 6845, Australia

4. Earth and Environmental Sciences Division, Los Alamos National Laboratory, Los Alamos, NM 87545, USA

Abstract

The Earth experienced global magmatic events correlated with the presence of supercontinents, suggesting that the distribution of continental pieces at the surface is fundamental. In most cases, the plume model is invoked to explain the presence of these large igneous provinces although some do not clearly show evidence for such mechanism. The aggregation of continent is known to have a significant effect on mantle convection and thermal evolution below continents, mostly enlarging the wave-length of convection and insulating the underlying mantle. Both processes tend to increase the temperature below the continental lithosphere, eventually triggering melting even without plume. This model, called mantle global warming, has been tested with convection models (Coltice et al., 2007). This paper questions the validity of this model in the past comparing predictions from numerical simulations to geological observations for continental flood basalts back to the Archean. The simulations predict the mantle global warming model could be an efficient mechanism to account for the peculiarities of magmatic provinces on Pangea, Rodinia and proposed Archean supercontinents like Kenorland and ZimVaalbara.

29 1. Introduction

30 The growth of the continental crust is an episodic process (Moorbath, 1978). One way to
31 identify pulses of continent formation is through the record of ages of zircons that carry the
32 informations about the generation of juvenile granites. In the available data, major growth
33 events are dated at 2.7, 2.5, 1.9, 1.1, 0.48, 0.28 and 0.1Ga, corresponding to mantle magmatism
34 and orogenic activity (Condie, 2004). Although no rock has been preserved from the Hadean,
35 4.1Gy old zircons of Jack Hills in the Ylgarn cratons suggest the presence of early continents
36 (Harrison et al., 2005).

37 Some of the major events, correlating with mantle volcanism, occurred when supercontinents
38 were aggregating or breaking up (Yale and Carpenter, 1998; Condie, 2004). Rodinia was
39 breaking up at 1.1Ga, Gondwana at 0.48Ga and Pangea was stable between 0.28 and 0.2Ga
40 before disrupting into the continents we see today. There are suggestions of Archean
41 supercontinents especillay between 2750-2650Ga (Aspler and Chiarenzelli, 1998) in a period of
42 rapid and worldwide formation of juvenile continental crust. The temporal coincidence between
43 supercontinents and widespread magmatism questions role of the distribution of continents in
44 trigerring large-scale mantle melting. Mantle convection studies have shown that continents can
45 impose their wavelength to the flow (Guilou and Jaupart, 1995; Phillips and Bunge, 2005)
46 which can lead to an increase in mantle subcontinental temperature (Grigné et al., 2007). Indeed
47 changing the wavelength changes the efficiency of heat removal as well. Another effect is to
48 insulate the subcontinental mantle and reduce the heat loss to very low values. Indeed, mantle
49 heat flow can be as low as 12mW m^{-2} within cratons (Jaupart et al., 2007), which impedes the
50 cooling of the underlying mantle. A consequence of insulation and wavelength change is that
51 continental aggregation leads to an increase in subcontinental temperature even without mantle
52 plumes. Numerical simulations of mantle convection suggest it could be as high as 100°C ,
53 triggering melting in the asthenosphere and eventually the lithosphere on a very widespread
54 area, as it is called the mantle global warming model (Coltice et al., 2007).

55 However, when plume exist they tend to start and focus below continents because it is a
56 naturally hot region (Gurnis, 1988; Zhong and Gurnis, 1993; Guilou and Jaupart, 1995; Phillips
57 and Bunge, 2005; Phillips and Bunge, 2007). For now, only the (super)plume model as been
58 invoked to explain the magmatic activity during continental growth pulses. In most cases, plume
59 evidence is very limited and some ambiguous geological proxies are used (Courtillot et al.,
60 1998). To account for a plume origin, several observations have to be made in the framework of

61 a plume paradigm: hotspot tracks, domal uplift, deep mantle isotopic fingerprint, restricted
62 geometry of magmatism, temperature excess (Sleep, 1990). Although, convection simulations
63 that take into account the dynamical effects of chemical heterogeneities in the source of plumes
64 show that this paradigm could be revised and a wide variety of thermo-chemical plumes could
65 exist within the mantle (Farnetani et al., 2005).

66
67 Some of the largest CFB on Earth do not display evidence for the plume model, even taking into
68 account some of the complexities of the thermo-chemical plumes. Off course, for most of the
69 geological record, the only traces of CFBs left are giant dikes or large-scale basaltic eruptions
70 from which recognition of a plume pattern is very difficult (Ernst and Buchan, 2002). It is only
71 with rocks of ages younger than 200My that the emplacement of CFBs can be more accurately
72 documented. But even in the recent record, some CFBs hardly match any plume criteria. One of
73 the best examples is the Central Atlantic Magmatic Province (CAMP): there is no hotspot track,
74 no geochemical fingerprint for deep mantle sources, no domal uplift, and it is so large-scale
75 ($>10^6$ km²) that a plume origin cannot be accounted for. In this case, the global warming model
76 fits well the observations (Coltice et al., 2007) and suggests that other CFBs in the past could be
77 too.

78 In this paper, we investigate the role of the mantle global warming model in generating
79 continental flood basalts on supercontinents over the Earth's history. We first explicit the model
80 and show 3D spherical simulations describing how the temperature changes in the
81 subcontinental mantle for variable continental covers that correspond to situations in the past.
82 These results allow us to propose some continental flood basalts over Earth's history that could
83 be explained by this model instead of plume models.

84 **2. The model**

85 2.1. Physics and phenomenology

86 There is a strong feedback between mantle convection and the evolution of the continental
87 distribution at the surface of the Earth. Cold downwellings draw continents by focusing
88 convergence while hot upwellings push them away. At the same time, the strength and insulating
89 power of continents strongly impede the presence of downwellings below them so they tend to
90 create hot regions. It has led Anderson (1982) to suggest that the geoid high within the Atlantic
91 is a remnant of hot mantle generated below Pangea for instance. Hence continental rafts play an

92 important role in the convective organization since they constitute mechanical and thermal
93 heterogeneities within the top boundary layer that drives most of the dynamics since heat from
94 the core probably does not exceed 25% of the global heat budget (Hernlund and Labrosse,
95 2007).

96
97 Aggregation and dispersal of continents are then fundamental in modifying the temperature
98 field in the mantle. A supercontinent has a pronounced insulating power and can force the flow
99 towards longer wavelength than with separate smaller continents. As a consequence, aggregated
100 continents have hotter sublithospheric temperature than when they are dispersed theoretically,
101 and this even if there is no heat coming from the core i.e. without hot plumes. In principle, a
102 mantle only heated from within (cooling and radiogenic heat) can display subcontinental
103 thermal excursions when continents aggregate and disperse. Coltice et al. (2007) used 2D and
104 3D mantle convection models with continental rafts to show the existence of such mechanism.
105 In their framework, they showed continental aggregation would generate a temperature increase
106 greater than 70°C in 100My when continents aggregate (with moving continents in 2D) in the
107 absence of heat from the core. However, the simulations contain simplifications like rigidity of
108 continents, linear rheology, and fixed continents for the 3D case. It is extremely challenging
109 today to use realistic rheologies (temperature, depth and stress dependent) in spherical models
110 that generate self-consistently a plate like behaviour (Tackley, 2000). The viscosity used in
111 numerical models could be crucial since there is a feedback between temperature, stress and the
112 flow through viscosity. In the following, we explore in simple spherical models the effects of
113 the size and distribution of continents to investigate how the mantle global warming model
114 could have worked in the past.

115 116 2.2. Numerical models

117 Modelling the thermal evolution of the convective mantle with continents involves several
118 ingredients. First, a physical and numerical model of mantle convection has to be used. Then a
119 physical formulation of continents has to be inserted consistently with the physical framework.
120 Interaction between mantle flow and continents has to be implemented without violating the
121 conditions of free convection in which self-organization is crucial. Hence, we solve the Navier-
122 Stokes equations for incompressible material with the code TERRA in 3D spherical geometry
123 (Bunge and Baumgardner, 1995). The viscosity is laterally constant but increases by a factor of

124 30 at the 660km boundary, as suggested by geoid and post-glacial rebound studies (Ricard et al.,
1 125 1993). A temperature and stress-dependent rheology is beyond the capabilities of present-day
2 126 numerical models for highly vigorous convection in spherical geometry. It is not worth to use
3
4 127 only temperature-dependence in the models since it would freeze the cold surface and generate
5
6 128 a stagnant lid that is not realistic to study the Earth (Christensen, 1984). The calculations involve
7
8 129 85% of heat from within (radioactivity) and 15% from the core. The Rayleigh number based on
9
10 130 the upper mantle viscosity is 10^7 here, which is supposed to be close to present-day convective
11
12 131 vigor.

13 132
14
15 133 The continents are simulated by rigid lids. Their thickness is 220km thick, consistently with the
16
17 134 thickness of stable continental lithosphere determined by geophysical observations (Artemieva
18
19 135 and Mooney, 2001). In this study, the lids are fixed and hence have a zero velocity, acting like
20
21 136 undeformable lithosphere. It is a rather crude model but more advanced representation of
22
23 137 deformable continental lithosphere involves numerical complexities (Lenardic et al., 2003)
24
25 138 which are sufficiently difficult that no spherical 3D model of deformable continent has been
26
27 139 published up to now. However, rigid continents simulate the first-order effects of thermal
28
29 140 insulation and mechanical strength on mantle convection, as in many other studies (Gurnis,
30
31 141 1988; Guilou and Jaupart, 1995, Lowman and Jarvis, 1999).

32 142
33

34 143 2.3 Simulations

35
36 144 The goal of the calculations with fixed continents is to explore the potential of the mantle global
37
38 145 warming model for a planet with smaller continents. Indeed, Archean and Proterozoic
39
40 146 continents could have been smaller than today and melting caused by subcontinental warming
41
42 147 after aggregation could be questioned. Models are run for several convective overturns in order
43
44 148 to obtain statistically steady-state values for the subcontinental temperature. The total
45
46 149 continental covers is varied between 10% and 30% of the Earth's surface with dispersed and
47
48 150 aggregated lids.

49 151
50

51 152 The temperature beneath supercontinents is always larger than beneath dispersed continents
52
53 153 whatever the total continental cover in the models. A widespread zone develops below the
54
55 154 continent because of insulation and long wavelength of the flow (Fig.1). Even with 15% basal
56
57 155 heating, plumes don't necessarily occur below the continents. We compute a temperature
58
59
60
61
62
63
64
65

156 difference between the supercontinent case and dispersed case and present a value which is
157 normalized to the average temperature at the base of the boundary layer (i.e. temperature at the
158 base of the oceanic lithosphere would be the equivalent). The temperature at statistically steady
159 state beneath a supercontinent is 5% larger for small continental cover (10% of the Earth's
160 surface), 10% for intermediate continental cover (20%) and up to 15% for a present-day
161 continental cover (see Fig.2). The larger the continental cover, the larger the temperature
162 difference between aggregated and dispersed case is. These numbers are not very dependent on
163 the Rayleigh number in our calculations. Increasing the size of continents increases both
164 insulation and flow wavelength which consequently increase the temperature. In our models, the
165 “oceanic” area (area without continent) is not influenced by the distribution of the continents
166 since the temperature at the base of the boundary layer is similar in the aggregated and
167 dispersed states.

168 Even if 5% temperature difference seems small, considering the temperature difference over the
169 boundary layer being around 1500K during the Archean (Jaupart et al., 2007), the warming up
170 would already be 75K which is significantly high to melt the mantle. With the continents
171 growing while the mantle is slowly cooling, the expected temperature increase after continental
172 aggregation increased slightly with time and probably remained between 50 to 150K since the
173 Archean according to our calculations.

174

175 **2.2.1.Global warming provinces: case studies**

176 The results of the models can be confronted to observations on various large igneous provinces
177 in the past that can difficultly be explained by the plume mode.

178

179 **2.3. Pangea provinces**

180 Pangea provides the best example to test the global warming versus mantle plume models,
181 because it is the last supercontinent, which assembly and break-up stories are relatively well
182 constrained. Its final stages of assembly occurred between 320 and 250 Ma (Cawood and
183 Buchan, 2007), while its dispersal progressively spread out from ca. 190 Ma (Sahabi et al.,
184 2004) and is still in progress. The characteristics of the CFBs associated with the break-up of
185 the Pangean supercontinent are better constrained, compared to those associated to previous

1
2
3
4
5
6
7
8
9
10
11
12
13
14
15
16
17
18
19
20
21
22
23
24
25
26
27
28
29
30
31
32
33
34
35
36
37
38
39
40
41
42
43
44
45
46
47
48
49
50
51
52
53
54
55
56
57
58
59
60
61
62
63
64
65

186 supercontinents, providing the best opportunity to test the global warming model as Pangea
187 evolves from a supercontinent configuration to the present-day continental dispersal.

188 Six CFBs were emplaced after the complete aggregation of Pangea and are therefore directly
189 linked to its break-up, recording a 170 My-long story of continental dismemberment: the Central
190 Atlantic Magmatic Province (CAMP) at 200 Ma, the Karoo at 180 Ma, the Parana-Etendeka at
191 130 Ma, the Deccan at 65 Ma, the North Atlantic Province at 60 Ma and the Ethiopia-Yemen at
192 30 Ma (Courtillet et al., 1999). It is generally accepted that the four youngest CFBs (Parana-
193 Etendeka, Deccan, North Atlantic, Ethiopia-Yemen) were emplaced in response to a mantle
194 plume head activity, while Pangea was already more or less largely dismembered. On the other
195 hand, the plume model has been questioned for the two oldest CFBs (CAMP and Karoo)
196 emplaced while Pangea was still a supercontinent, corresponding to a geodynamic setting more
197 favorable to the global warming model.

198 Hereafter, some key-points considered as critical for the plume versus global warming models
199 will be (re)-examined for the CAMP and Karoo CFBs. These points concern mainly the size and
200 shape of the CFB province and the volume of erupted magmas, the presence or absence of a
201 hot-spot track, the geometry of the dyke swarms, the timing of magmatism, the chemical
202 composition of the magmas.

203

204 *3.1.1 The CAMP case (200Ma)*

205 The CAMP is the largest CFB on Earth, now extending on four continents (Europe, Africa,
206 North America and South America) and covering ca. 10^7 km² (Fig.3). It consists of a) huge sills
207 and some layered intrusions, mainly developed in West Africa and Brazil (Deckart et al., 1997,
208 Marzoli et al., 1999), b) elongated isolated dykes (up to 800 km long) mainly occurring in North
209 Africa, Europe and Canada (Bertrand, 1991; McHone et al., 2005) and dense dyke swarms,
210 along Eastern North America margin, in West Africa and Guyana (Dupuy et al., 1988; Deckart
211 et al., 1997; Verati et al., 2005; McHone et al., 2005), c) some lava flows remnants preserved in
212 Triassic basins in Portugal, Morocco, Eastern North America, Brazil and Bolivia (Bertrand et
213 al., 1982; Puffer, 1992; Marzoli et al., 1999, 2004; Bertrand et al., 2005; Verati et al., 2007). The
214 lava piles are 10 to 450 meters thick. The CAMP CFB mainly extends over the peri-cratonic
215 panafrikan to hercynian belts and intra-cratonic basins (Brazilian and West-African cratons).

216 All the volcanics and intrusive bodies are basaltic to gabbroic, respectively, except a few
217 ultramafic cumulates. The rocks are dominantly low-Ti tholeiites (Bertrand, 1991), except a few

18 high-Ti tholeiites restricted to a limited area in Liberia, Guyana and Brazil (Dupuy et al., 1988;
19 De Min et al., 2003; Deckart et al., 2005).

20 The CAMP is the oldest CFB which postdates by several tens million years the ultimate
21 aggregation of Pangea. It is associated with the earliest disruption of the supercontinent,
22 initiating the central Atlantic Ocean as far as ~190 Ma ago (Sahabi et al. 2004). The peak
23 igneous activity, established by recent $^{40}\text{Ar}/^{39}\text{Ar}$ dating (~70 reliable plateau ages), is around
24 199-200 Ma and coincides with the Triassic-Jurassic boundary (Marzoli et al., 1999, 2004;
25 Hames et al., 2000; Knight et al., 2004; Verati et al., 2007), taking into account ~1% bias
26 between $^{40}\text{Ar}/^{39}\text{Ar}$ and U/Pb chronometers (Schaltegger et al., 2008). Late minor activity seems
27 to persist up to 190 Ma (Deckart et al., 1997; Marzoli et al., 1999; Nomade et al., 2007).

28 The origin of the CAMP has been assigned by several authors to a mantle plume head
29 impingement beneath the lithosphere (Hill, 1991; Wilson, 1997; Oyarzun et al., 1997; Leitch et
30 al., 1998; Courtillot et al., 1999; Janney and Castillo, 2001; Ernst and Buchan, 2002), yet this
31 model has been refuted by others (McHone, 2000; De Min et al., 2003; Beutel et al., 2005;
32 Deckart et al., 2005; McHone et al., 2005; Verati et al., 2005) who favor a shallow mantle
33 origin. Several lines of evidence challenge the plume model:

34 - No hotspot tracks have been recorded on the Atlantic ocean floor as it was opening (McHone,
35 2000; McHone et al., 2005).

36 - The geometry of the CAMP is not consistent with the plume head model which predicts a
37 radial spreading over an equant area 2000-2500 km across (Campbell and Griffiths, 1990),
38 whereas the CAMP is much more extended (Fig...) along a ~8000 km area elongated from
39 Brittany, France (Jourdan et al., 2003) to Bolivia (Bertrand et al., 2005). This distribution is
40 more likely controlled by pre-existing lithospheric heterogeneities and weakness zones.

41 - To account for the elongated geometry, a northward channeling of the plume head has been
42 invoked, starting from the center of the hypothetical plume head inferred to be located close to
43 the Blake Plateau (Wilson, 1997; Oyarzun et al., 1997), yet this scenario is invalidated by the
44 absence of northward age propagation. On the contrary, if any migration of the magmatic
45 activity exists, it would rather propagate southward (Baksi, 2003; Nomade et al., 2007).

46 - Contrasting to its wide surface, the CAMP is characterized by a relatively low rate of magma
47 supply (mean thickness of volcanic sequences of 100-300 m) compared to the much thicker lava
48 piles observed in plume-related CFBs, such as Deccan or Ethiopian traps. The preservation of
49

1
2
3
4
5
6
7
8
9
10
11
12
13
14
15
16
17
18
19
20
21
22
23
24
25
26
27
28
29
30
31
32
33
34
35
36
37
38
39
40
41
42
43
44
45
46
47
48
49
50
51
52
53
54
55
56
57
58
59
60
61
62
63
64
65

249 thin lava units interstratified into sedimentary levels precludes that important volumes of lavas
1 250 might have been removed by erosion.
2
3 251 - The area near the Blake Plateau does not show evidence of uplift that would be expected if a
4
5 252 plume head had impinged the lithosphere (McBride, 1991; McHone, 2000).
6
7 253 - The apparent radial pattern of feeder dyke swarms first shown by May (1971), that would
8
9 254 account for the impingement of a plume head (Hill, 1991; Wilson, 1997; Leitch et al., 1998;
10
11 255 Ernst and Buchan, 2002), is a misleading oversimplification that ignores the regional geology:
12
13 256 a) Some dykes do not exist, e.g. the ENE-WSW dyke swarm repeatedly reported in SE
14
15 257 Mauritania (Hill, 1991; Leitch et al., 1998; Ernst and Buchan, 2002) corresponds to faults, not to
16
17 258 dykes (1:1000000 geological map of Mauritania, 1975). In addition, the subsurface dyke swarm
18
19 259 displaying the same trend in Senegal is hypothesized from magnetic survey, yet its existence and
20
21 260 “a fortiori” its age are unknown. Therefore, this ENE-WSW to E-W branch of the radial dyke
22
23 261 pattern is not constrained.
24
25 262 b) Some dykes that would fit the radial pattern (e.g. NE-SW dykes in northern CAMP) display
26
27 263 inherited trends reactivated during the CAMP event rather than neo-formed trends imposed by a
28
29 264 plume head impact. Other dyke swarms (e.g. in Guyana-Surinam) include both Proterozoic and
30
31 265 CAMP dykes (Deckart et al., 1997, 2005). On the other hand, the dyke swarm intruding the
32
33 266 Reguibat shield in NW Mauritania is poorly dated, but provided so far only Proterozoic ages
34
35 267 (Dosso, 1975).
36
37 268 c) Some dyke swarms are much more complex than shown on the “radial pattern”. For exemple,
38
39 269 the Taoudenni dyke swarm in northern Mali comprises more than 800 dykes among which only
40
41 270 a few fit the NE-SW trend that would be expected in this area in a radial pattern (Verati et al.,
42
43 271 2005). Similarly, the eastern North America coastal dykes cannot be reduced to those which fit
44
45 272 the radial pattern, as they show multiple orientations and cross-cutting relationships which
46
47 273 reflect a changing regional stress field (Beutel et al., 2005; McHone et al., 2005)
48
49 274 - The chemical and isotopic compositions of CAMP basalts are diagnostic of shallow-mantle
50
51 275 sources and do not bear a deep plume composition. The predominating low-Ti group is
52
53 276 characterized by negative Nb-Ta anomalies, enrichment in large ion lithophile elements (LILE)
54
55 277 relative to high field strength elements (HFSE) and Nd-Sr isotopic compositions diagnostic of
56
57 278 lithospheric sources formerly enriched by ancient subduction processes (Bertrand et al., 1982;
58
59 279 Bertrand 1991; Pegram 1990; Puffer, 2001; Cebria et al., 2003; De Min et al., 2003; Deckart et
60
61 280 al., 2005; Verati et al., 2005). The subordinate high-Ti group, chemically and isotopically
62
63
64
65

281 distinct, indicates the contribution of the asthenospheric mantle (Dupuy et al., 1988; Deckart et
282 al., 2005).
283 None of the CAMP areas on which Nd-Sr-Pb isotopes were investigated so far (Pegram, 1990;
284 Jourdan et al., 2003; Cebria et al., 2003; Deckart et al., 2005) bear the HIMU signature
285 diagnostic of the mantle plumes (Cape Verde, Fernando do Noronha, Asuncion) which might
286 have been in a favorable position in late Triassic times to trigger the CAMP magmatism
287 (Morgan, 1983).

288

289 *3.1.2 The Karoo case (180Ma)*

290 The Karoo CFB extends over more than 3×10^6 km², from southern South Africa to Malawi and
291 from western Namibia to Mozambique, with minor outcrops in Antarctica (Fig.4). It postdated
292 the CAMP by about 20 My and is associated to the second phase of the Pangea fragmentation,
293 corresponding to the break-up of southern Gondwana leading to the opening of the SW Indian
294 Ocean and Southern Ocean. The Karoo CFB consists of a vast cover of lava flows and sills,
295 giant dyke swarms and more localized intrusive centers, intruding the Archean Kaapvaal-
296 Zimbabwe cratons, the Proterozoic Limpopo belt and the Permian-Jurassic Karoo sedimentary
297 basins.

298 Karoo lavas remnants consist of: a) tholeiitic basalt lava piles in Lesotho (Marsh et al., 1997), in
299 Botswana and adjacent Zambia-Zimbabwe (Wigley, 1995; Jones et al., 2001; Jourdan et al.,
300 2005) and in central Namibia (Duncan et al., 1997); b) the ~ 10 km-thick Lebombo lava pile
301 (Cox, 1992; Watkeys, 2002) comprising an upward succession of nephelinites, picrites, tholeiitic
302 basalts and rhyolites (Sweeney et al., 1994). Picrites and basalts also occur in the Tuli and
303 Mwenezi basins (Cox, 1992). Several gabbroic to granitic intrusive complexes also intrude the
304 latter basin (Jourdan et al., 2007a). Vast tholeiitic dolerite sills are intruded at various
305 stratigraphic levels in several Karoo basins, particularly in South Africa (Jourdan et al., 2008),
306 but also in south-eastern Namibia, in southern Botswana and in Mozambique. The main dyke
307 systems are the N110° Okavango dyke swarm, the N70° Save-Limpopo dyke swarm and the N-S
308 Lebombo and Rooi Rand dyke swarms, forming, together with the associated rifts, a pseudo-
309 radiating system (Fig.), i.e. the so-called Karoo triple junction (Burke and Dewey, 1972;
310 Campbell and Griffiths, 1990; Ernst and Buchan, 2002).

311 A comprehensive ⁴⁰Ar/³⁹Ar dating campaign (~90 reliable plateau ages) shows that the main
312 volume of the basaltic sequence was emplaced over 3 to 4.5 Ma around 180 Ma, whereas the

1 313 entire province sustained activity over a total of ~10 Ma, from 184 to 174 Ma (Jourdan et al.,
2 314 2005, 2007a, 2007b). The increase of magmatic activity seems to coincide with the
3 315 Pliensbachian-Toarcian minor biotic crisis (Jourdan et al., 2008).

4 316 Since the pioneering work of Burke and Dewey (1972), the Karoo CFB is repeatedly referred to
5 317 as an example of plume related CFB (e.g. Campbell and Griffiths, 1990; Courtillot et al., 1999;
6 318 Ernst and Buchan, 2002). One of the main argument supporting this plume model was the
7 319 presence of the so-called triple junction supposed to have been triggered by the impact of a
8 320 mantle plume head beneath the southern Africa lithosphere in Jurassic times, despite the lack of
9 321 dating on the related dyke swarms. Recent $^{40}\text{Ar}/^{39}\text{Ar}$ dating performed on the N110° Okavango,
10 322 N70° Save-Limpopo and N-S Lebombo dyke swarms (forming the “triple junction”), combined
11 323 to geochemical analyses, reveal that these dyke swarms unambiguously include Proterozoic
12 324 dykes (Jourdan et al., 2004, 2006). For instance, the N110° Okavango dyke swarm includes 12%
13 325 of Proterozoic dykes (Jourdan et al., 2004). In addition, a structural analysis strongly suggests
14 326 that Karoo dyke orientations are largely controlled by pre-existing structures that also controlled
15 327 emplacement of Precambrian dykes (Jourdan et al., 2006). The apparent triple junction
16 328 geometry was not induced by the arrival of a mantle Karoo plume head but is inherited from
17 329 previous history of the Kaapvaal and Zimbabwe cratons. Therefore, this “triple junction” should
18 330 no longer be used as an argument for demonstrating (although it does not exclude) the existence
19 331 of a Karoo mantle plume.

20 332 Another reason why the Karoo mantle plume may be questioned is the lack of volcanic track
21 333 linking the Karoo CFB with a present day hot spot, which position vary (Crozet, Marion,
22 334 Bouvet ...) depending of the authors (Morgan, 1981; Richards et al., 1989; Hawkesworth et al.,
23 335 1999).

24 336 The involvement of a deep mantle plume in the genesis of Karoo CFB is also questioned on the
25 337 basis of geochemical arguments. Only a few geochemical studies conclude that a mantle plume
26 338 does contribute to the chemical composition of the Karoo magmas (Ellam and Cox, 1992).
27 339 Based on isotopes and trace elements patterns (LILE/HFSE enrichment), most geochemical
28 340 investigations argue for melting of heterogeneous old sub-continental lithospheric mantle
29 341 (SCLM) (Duncan et al., 1984; Hawkesworth et al., 1984; Ellam and Cox, 1989; Sweeney and
30 342 Watkeys, 1990; Elburg and Goldberg, 2000) or mixing between lithospheric and asthenospheric
31 343 mantle sources (Sweeney et al., 1991; Ellam and Cox, 1991; Sweeney et al., 1994). More
32 344 recently, two scenarios have been proposed, involving either the polybaric melting of SCLM or

345 mixing between SCLM and an asthenospheric or deeper OIB-like mantle plume (Jourdan et al.
346 2007c). Regardless of which of the two scenarios is invoked, the spatial distribution of the low-
347 and high-Ti magmas matches the relative positioning of the cratons and the Limpopo belt in
348 such a way that strong control of the lithosphere on magma composition and distribution is pre-
349 requisite of any petrogenetic model applied to the Karoo CFB (Sweeney and Watkeys, 1990;
350 Jourdan et al., 2007c).

351

352 2.4. Rodinia provinces

353 Similarly to Pangaea, the assembly and breakup of the Proterozoic mega continent Rodinia was
354 accompanied by the emplacement of major LIPs and dyke swarms (e.g. Ernst and Buchan,
355 2001; Ernst et al., 2005, 2008). Most of these LIPs are only scarce remnant occurring as sills
356 and dyke swarms as the lava flow components have been in most cases eroded. Furthermore,
357 Proterozoic LIPs is challenging because of significant alteration and anchizone up to green shist
358 facies metamorphism affecting the samples.

359 From 1.3Ga until its final assembly (~900 Ma; Li et al., 2008) and subsequent breakup, Rodinia
360 have been the witness of many LIP events (e.g. Ernst et al., 2008). Of particular interest, is a
361 cluster of LIPs around 1.1 Ga (Fig. 5) as the surface covered by each of the provinces remnants
362 is of several 10^6 km². This makes these provinces equivalent in size to the Pangean provinces
363 mentioned previously.

364 Hereafter, we will focus on three major provinces (Umkondo, Keweenawan and Warakurna)
365 emplaced sub-synchronously at ~1.1 Ga during the assembly of Rodinia (Fig. 5). According to
366 recent paleocontinent reconstructions, Rodinia was not complete before ca 900 Ma (e.g. Li et
367 al., 2008) and the 1.1-Ga configuration allow us to test our model further on a partially
368 assembled mega continent (Fig. 5).

369

370 3.2.1. *The Umkondo case (1.1Ga)*

371 Paleomagnetical and geochronological (mainly zircons U/Pb analyses) investigations permit to
372 attribute a common origin to Proterozoic tholeiitic rocks occurring throughout northern South
373 Africa, Botswana, Zimbabwe and possibly Antarctica (Hanson et al., 2004). This province is
374 now called Umkondo based on the name of Umkondo Zimbabwe dolerite formation of the same
375 age. (Hanson et al., 1998). This province consists of tholeiitic mafic intrusions (sills and dykes
376 swarms, e.g. Jourdan et al., submitted) and scarce remnants of eroded basaltic lava-flows

377 emplaced over an estimated paleo-surface of $\sim 2.5 \cdot 10^6$ km² (Hanson et al., 2004). Robust ages
378 clustering around 1108 ± 3 Ma have been obtained using zircon and baddeleyite U/Pb TIMS
379 technique suggesting a relatively short duration of the magmatism. Umkondo LIP is therefore
380 synchronous with the Rodinia mega-continent formation (Hanson et al., 1998; Dalziel et al.,
381 2000) and in particular the Laurentia and Kalahari craton collisions (Kibaran Grenville-Llano
382 and Namaqua-Natal Orogenies; 1.4-1.0 Ga). The “Kibaran” (Namaqua-Natal) Mesoproterozoic
383 belt that occurs over 3000 km long through central and southern Africa. Between 1.4 and 1.0
384 Ga, Kibaran metasedimentary and igneous rocks were involved into two compression events
385 (Johnson & Oliver, 2000) including an active continental margin followed by a continental
386 collision.

387 The majority of the rocks underwent green schist metamorphose and alteration, but their
388 composition is not modified beyond the point they can be used to study petrogenetic processes
389 (Munyanyiwa, 1999). The UIP dolerites are not well studied, but studies carried out so far shat
390 that they mostly consist of low-Ti basaltic rocks, as commonly found in many LIPs. Umkondo
391 dolerites have a strong lithospheric signature as shown by a strong Nb anomaly ($Nb/Nb^*=0.2-$
392 0.4) and low Ce/Pb (2 to 7) ratios (Jourdan et al., submitted). The province is not associated
393 with any hot spot track. No evidence of magmatic contribution from a mantle plume is
394 recognized in the samples analyzed so far (e.g. Hanson et al., 2006; Jourdan et al., submitted).
395 Similar composition with the spatially overlapping 180-Ma Karoo province suggest that both
396 provinces are likely to originate from a very similar mantle source. The source have been only
397 slightly modified since the extraction of the Umkondo basalts and Jourdan et al. (submitted)
398 proposed that the source should be “attached” to the African plate and therefore preferentially
399 located in subduction-metasomatised sub-continental lithospheric mantle.

400

401 *3.2.2 The Laurantian large igneous provinces (1.1-1.07 Ga)*

402 The Laurantian provinces as defined hereafter includes the Keweenawan “mid-continental rift”
403 ($\sim 2 \cdot 10^6$ km²; Cannon, 1992) and the South Western U.S. diabase ($\sim 0.4 \cdot 10^6$ km²; Ernst et al.,
404 2008) provinces.

405 Both provinces have been emplaced sub-synchronously with still scarce U/Pb ages ranging
406 from ca 1.11 to 1.09 Ga for the former (e.g. Vervoort et al., 2007) and from ca 1.10 Ga to 1.07 Ga
407 (e.g. Heaman and Grotzinger, 1992; Ernst and Buchan, 2001 and reference therein) for the latter.
408 The Keweenawan province is the best studied of the two Laurantian provinces and is a bimodal

409 province including mafic (typically olivine tholeiites; Paces and Bell, 1989) and minor silicic
410 (Vervoort and Green, 1997; Vervoort et al., 2007) rocks. Element and Sr-Nd-Pb isotope
411 geochemistry studies done so far indicate that the magma is derived from enriched mantle
412 reservoirs (Shirey et al., 1994) and share common features with LIPs like Umkondo and Karoo.
413 For example, both Karoo and Keweenawan eruptive sequence have an early activity represented
414 by picrites with a strong lithospheric signature (Shirey et al., 1994; Jourdan et al., 2007). The
415 mantle sources proposed to explain the origin of this problem comprise a variety of scenario
416 ranging from asthenospheric/subasthenospheric mantle plume to enriched lithospheric mantle (or
417 a combination of both), altogether with variable degree of crustal contamination (e.g. Paces and
418 Bell, 1989; Nicholson and Shirey, 1990; Vervoort et al., 2007 and references therein). Crustal
419 contamination affects mostly the silicic rocks that derive partially from the fusion of the
420 Archean crust (Vervoort et al., 2007). The South Western U.S. diabase are much less studied
421 and mostly geochronology and paleomagnetic data are available (e.g. Shastri et al., 1991;
422 Heaman and Grotzinger, 1992; Ernst & Buchan, 2001; Ernst et al., 2008). This province consists
423 mostly of up to 450m-thick doleritic sills and no chemical data has been published to our
424 knowledge. This currently makes it difficult to correlate with other LIPs.

425

3.2.3 *The Warakurna large igneous province (1.05Ga)*

427 This province regroups coeval magmatism distributed over $\sim 2.5 \cdot 10^6$ km² and distributed mostly
428 over Western and northern Australia (Wingate et al., 2004). It is represented mostly by silicic
429 and basaltic lava flows and mafic and ultramafic intrusions. The age of the province has been
430 determined using zircon SHRIMP U/Pb technique and yielded a mean age of 1076 ± 3 Ma
431 although minor magmatism intrusion continue until ~ 1050 Ma. Investigation using the more
432 robust CA-TIMS analysis would be desirable to obtain a more accurate estimate of the age along
433 with a better estimation of the magmatism duration. Nevertheless, an age of ~ 1080 Ma makes
434 the Warakurna province synchronous with the Pinjarra orogen, Western Australia (Wingate et
435 al., 2004; Bruguier et al., 1999; Cobb et al., 2001) and may indicate a causal relationship
436 between the Pinjarra subduction and emplacement of the Warakurna magmatic province.

437 The rocks consist of dolerite with sericitized plagioclase and amphibolitized pyroxene and show
438 an enriched tholeiitic composition with SiO₂ ranging from 48 to 55 wt%. They are enriched in
439 LILE and show strong Nb anomaly that Zhao and McCulloch (1993) and Glikson et al. (1996)
440 attributed to the melting of subduction-modified lithospheric mantle. Zhao and McCulloch

1
2 442 (1993) invoked a rising mantle plume to explain the thermal anomaly required to melt the
3 SCLM. No mantle plume track has been found suggesting that the role of a mantle plume, if
4 any, was confined as heat purveyor.
5
6 444

7 445 2.5. Archean provinces

9 446 Looking for CFBs caused by global warming beneath supercontinents is a difficult task because
10 of the intrinsic difficulties of working on such old rocks. Although, the magmatic evolution of
11 the mantle within the first couple of billion years involved sudden and violent crises, possibly
12 mantle overturns and/or superplume events (Stein & Hofmann, 1994; Breuer & Spohn, 1995;
13 Barley et al., 1998; Condie, 2001), that punctuated periods of relative quietness. In this context,
14 the period between 2.75 and 2.65 Ga is one of the most dramatic in the Earth's history. In that
15 period, most Archaean cratons were covered by 5 to 15 km thick, komatiite-bearing, basalt
16 dominated, greenstone covers (Nelson, 1998), while isotopic age distribution of detrital zircons
17 point to a major peak production of juvenile continental crust (Gastil, 1960; Condie, 2001; Rino,
18 2004). In many cratons, this event preceded and overlapped with a profound episode of crustal
19 anatexis and differentiation (Rey et al., 2003). Although partial of melting of volatile-rich
20 mantle above a subduction zone can generate komatiites, the geochemistry of most late
21 Archaean komatiites demand a deep source origin and request either a large melt fraction (50%)
22 or the partial melt of a depleted mantle source (Arndt, 2003). Considering the global character
23 of the late Archaean crisis, a superplume event is indeed very appealing (Isley and Abbott,
24 1999; Condie 2004; Barley et al., 1998), however, it is not without problems. In this section, we
25 review the extent of the late Archaean volcanism and the problems linking this volcanism to
26 superplumes.
27
28 464

29 465 3.3.1. *Surface extent of the 2.75-2.65 Ga magmatic crisis*

30 466 In the Kaapvaal Craton, the up to 8 km thick Ventersdorp extends over 3e5 km² (van der
31 Westhuizen et al. 1991, Eriksson et al., 2002) and includes 2.72 Ga to 2.69 Ga old subaerial
32 continental komatiitic basalts, tholeiitic basalts and sedimentary rocks (Armstrong et al, 1991),
33 that precedes and overlaps with crustal melting, plutonism and coeval sedimentation (Schmidz
34 and Bowring, 2003).
35
36 470

37 471 In the Zimbabwe craton, the base of the 2.7 Ga old craton wide Ngezi Group includes the
38 Zeederberg continental flood basalt, which covers an area over 2.5e5 km² (Prendergast, 2001).
39
40
41
42
43
44
45
46
47
48
49
50
51
52
53
54
55
56
57
58
59
60
61
62
63
64
65

1 473 Its base is made of the submarine Reliance formation, which includes up to 2km thick
2 474 interlinked komatiite sills extending over 100 km intercalated within sandstones and pillowed
3 475 basalts (Prendergast, 2001). This event precedes and overlaps with Sesombi-Wedza granitoids
4 476 emplaced between 2.7 and 2.65 Ga.

5 477 The evolution of the Superior Province culminated between 2.75 and 2.7 Ga with the
6 478 emplacement of submarine magmatism involving komatiites before craton-scale crustal anatexis
7 479 and plutonism, the bulk of which occurred between 2.71 and 2.66 Ga.

8 480 In the Slave Province, the 2.74 to 2.69 Ga Yellowknife greenstone belt includes up to 6 km thick
9 481 pillowed and massive flow of tholeiitic basalts, minor komatiites and rhyolitic tuff intercalations
10 482 (Bleeker, 2005). This volcanic event, which covers $> 10^5$ km² (Bleeker, 2005), was followed
11 483 from 2.69 to 2.66 Ga by calc-alkaline volcanism and Tonalite-Trondhjemite-Granodiorite
12 484 plutonism (Bleeker, 2005).

13 485 In the East goldfield province of the Yilgarn Craton, a 12 ± 2 km thick package ($>10^5$ km²) of 2.72
14 486 to 2.70 Ga marine tholeiite–komatiite and tholeiite–calc-alkaline associations (Barley, et al.,
15 487 1998) is followed by episodic deep-water volcanoclastic sedimentation from to 2.70 to 2.66 Ga
16 488 coeval with craton-scale crustal anatexis.

17 489 In the Pilbara craton, all the older units are unconformably overlain by the mainly subaerial
18 490 Fortescue Group (2.765–2.687 Ga) (Nelson et al., 1992; Blake, 1993; Arndt et al., 2001; Blake,
19 491 2001). The Fortescue, which covers at least $1.8\text{e}5$ km² (Eriksson et al., 2002), is made of ca. 7
20 492 km thick volcanics which includes a series of tholeiitic basalts, minor komatiites, felsic
21 493 volcanics and clastics rocks (Hickman, 1983; Thorne and Tyler, 1997; Thorne and Hickman,
22 494 1998; Blake, 2001).

23 495 Greenstones emplaced at 2.7 Ga have also been described in the Wyoming craton (e.g.
24 496 Stillwater intrusion), Dharwar craton (e.g. Ramagiri-Hungund composite greenstone belt,
25 497 Gadwal greenstone belt)

26 498

27 499 *3.3.2. Models for the 2.75–2.65 Ga magmatic crisis*

28 500 In all the above cratons, 1/ the synchronicity of bimodal volcanism, felsic plutonism and
29 501 sedimentation, 2/ the calc-alkaline composition of some basalts, despite minor komatiites, and
30 502 3/ the syn- to late-contractinal deformation, have lead to interpretative models involving
31 503 multiple subduction zones and discrete back-arc basins between micro-plates. The collisional
32 504 aggregation these micro-plates finally led to the formation of late Archaean cratons. This model

33
34
35
36
37
38
39
40
41
42
43
44
45
46
47
48
49
50
51
52
53
54
55
56
57
58
59
60
61
62
63
64
65

505 has been proposed for the late Archaean of the Yilgarn craton (Myers, 1993; Swager et al., 1997;
506 Barley et al., 1989, 1998); the Superior Province (Corfu, 1987; Percival and Williams, 1989;
507 Card, 1990; Ludden et al., 1993; Wyman et al., 2002); the Slave Province (Kusky, 1989; 1990);
508 the Zimbabwe craton (Dirks and Jelsma, 1998; Jelsma and Dirks, 2002; Horstwood et al., 1999);
509 and the Kaapvaal craton (REF). Yet, in all the above cratons, detailed field studies have noted
510 the strong coherence of the greenstone stratigraphy across so-called terrane boundaries as well
511 as the lack of crustal scale features validating collisional tectonics. This prompted the
512 proposition of an alternative model based on the emplacement of craton-scale continental flood
513 basalts, a model which has been proposed in the Slave province (Bleeker et al., 1999a, 1999b),
514 Zimbabwe (Prendergast, 2001; Wilson, 1979), in the Superior Province (Heather et al., 1995;
515 Heather, 1998; Ayer et al., 1999, 2002; Thurston, 2002; Benn, 2006), and the Yilgarn (Rey et al.,
516 2003). The profound phase of crustal anatexis that overlapped and post-dated continental flood
517 basalts in many cratons could be linked to the thermal insulation effect associated with the
518 emplacement the thick greenstones cover on a radiogenic crust (Rey et al., 2003). It is worth
519 noting that recent Hafnium isotopes data on zircon show that, contrarily to the 3.3 Ga and 1.9
520 Ga events, the large anomaly in the isotopic age distribution of zircons is not accompanied with
521 the formation of juvenile crust (Kemp et al., 2006). Intra-crustal anatexis alone, rather than the
522 formation of juvenile crust in a subduction zones, could explain the isotopic age distribution of
523 detrital zircons as well as the change of the average composition of emerged landmasses
524 recorded in black shales (Taylor and McLennan, 1985; Rey and Coltice, 2008).

525

526 *3.3.3. The cause of the 2.75-2.65 Ga volcanic crisis: Plume vs mantle global warming*

527 Hitherto, only mantle plumes were considered a viable setting of deep mantle partial melting.
528 The application of the superplume model in the late Archaean is not without problem.

529 1/ Most plume-related Phanerozoic continental flood basalts were emplaced over a very short
530 periods typically less than a few Myr. In contrast, the late Archaean continental flood basalts
531 were emplaced over a few tens of Myr.

532 2/ Subduction-related calc-alkaline volcanism is often spatially and temporarily associated with
533 komatiites. Although, models have been proposed to explain the production of komatiitic
534 magma in a subduction setting, most late Archaean komatiites did not form in a subduction zone
535 (Arndt, 2003). This leads to very complex tectonic models involving coeval upwelling flow
536 (plume) and downwelling mantle flow (subduction), both in the same location.

1 537 3/ Komatiite in Archaean CFB are generally less than 5% (Viljoen & Viljoen 1969 de Wit &
2 538 Ashwal 1997) and the bulk of continental flood basalt are made of basalt involving lower
3
4 539 degrees of melting. On that argument, large partial melt of a deep fertile plume could be ruled
5
6 540 out in favor of a smaller melt fraction in a refractory upper mantle source.

7 541 4/ In the Yilgarn, the geochemistry of 2.72-2.68 Ga basalts indicates extraction from a depleted
8
9 542 mantle with evolution from residual-plagioclase to residual-garnet. This suggests that
10
11 543 komatiites and basalts in the Eastern goldfield province derived from melting that took place at
12
13 544 progressively greater depths (Bateman et al., 2001). Interestingly, the same conclusion was
14
15 545 proposed in the Pilbara to explain the increase in FeO and incompatible elements in
16
17 546 progressively younger terms of the Fortescue Group (Arndt, 2001). In the context of a rising
18
19 547 plume, the downward migration of the melting source is not clear.

20
21 548 Mantle global warming above aggregating continents could provide a viable alternative to
22
23 549 surperplume events. Williams et al. (1991) proposed that a supercontinent, Kenorland, formed
24
25 550 at around the 2.7 Ga via the aggregation of the North American shields (the Slave Province,
26
27 551 Superior Province, Wyoming craton), joined perhaps by the Baltic and Siberian shields
28
29 552 (Bleeker, 2005). A possible second supercontinent, the Zimvaalbara, may have included the
30
31 553 Yilgarn craton, the Pilbara craton, The Gawler craton, the Zimbabwe craton, the Kaapvaal
32
33 554 craton, the Congo craton, the São Francisco craton, and possibly the Dharwar craton (Aspler
34
35 555 and Chiarenzelli, 1998). It is not clear how mantle plumes could have dominated the mantle
36
37 556 flow beneath supercontinents at the stage of their aggregation. In contrast, we showed that the
38
39 557 formation of such supercontinents could trigger the progressive warming of the sub-continental
40
41 558 mantle. The mantle global warming model involves a mantle scale upwelling to explain the
42
43 559 occurrence of komatiite. Therefore, there is no need to invoke complicated models involving
44
45 560 mantle plumes impinges on a subducting slabs to explain the intercalation of komatiites with
46
47 561 basalts.

48
49 562 Although most late Archaean continental flood basalts emplaced onto flooded continents, the
50
51 563 Pilbara and the Kaapvaal cratons were largely emerged at the time of volcanism. Therefore,
52
53 564 although continental emergence was not yet the rule, global high sea level is not expected in the
54
55 565 mantle warming model as mantle warming doesn't affect oceanic areas.

56
57 566 Due to the progressive warming of the sub-supercontinental mantle, the mantle geotherm would
58
59 567 cross the mantle solidus at a progressively increasing depth. This could explain the progressive
60
61
62
63
64
65

1 568 deepening of the melting source as recorded by the Komatiites from the Yilgarn cratons
2 569 (Bateman et al., 2001) and the Pilbara craton (Arndt, 1999).

3
4 570 Finally, the process of mantle warming and melting underneath insulating supercontinent is
5
6 571 similar to crustal warming and anatexis due to thermal insulation of the craton under greenstone
7
8 572 cover proposed in the Yilgarn (see Fig.6) by Rey et al. (2003). Therefore, the late Archaean
9
10 573 volcanic crisis and plutonic crisis can be seen in a broad context of nested insulation processes.

11
12 574

13 14 15 575 **2.5.1. Conclusions**

16
17
18 576 The presence of a supercontinent at the surface of the Earth has a major impact on the
19
20 577 convective flow within the mantle, as shown by our 3D spherical convection simulations. As a
21
22 578 consequence, the subcontinental temperature is 5-15% higher than for cases with dispersed
23
24 579 continents. The smaller the continental cover, the smaller is the temperature increase with
25
26 580 aggregation. For a continental cover larger than 10% of the Earth's surface, it is expected that
27
28 581 the subcontinental mantle could warm by more than 70K over an area comparable to the size of
29
30 582 the supercontinent. The mechanism of mantle global warming, alternative to mantle plumes, is
31
32 583 then a viable hypothesis for the origin of some continental flood basalts since the Archaean.

33
34 584 The numerical models are used to explore realistic physical mechanism from which quantitative
35
36 585 predictions can be made and tested against data. In the framework of the mantle global warming
37
38 586 model, the models predict that

- 39
40
41 587 – the temperature increase causing melting does not exceed more than 100K
- 42
43
44 588 – heating occurs over an area comparable to the supercontinent
- 45
46
47 589 – magmatic sources are mostly asthenosphere and continental lithosphere
- 48
49
50 590 – melt extraction is controlled by tectonics.

51
52
53 591 The mantle global warming model is consistent with the observations made on some CFBs in
54
55 592 the geological record. The best example is the CAMP (200Ma), the largest magmatic province
56
57 593 on Earth in area, but more and more evidence point also to the Karoo (180Ma). On the basis of
58
59 594 geochronology, geochemistry and tectonics, we suggest that during the Proterozoic, the

60
61
62
63
64
65

595 Umkondo, Laurentian and Warakurna CFBs are derived from mantle global warming beneath
596 the Rodinia supercontinent around 1.1Ga. The global magmatic crisis around 2.7Ga in the
597 Archean could also be explained by heating below the formation of Kenorland and Zimvaalbara
598 supercontinents, for which plumes are difficult to invoke.

599

600 **References**

601 Anderson, D.L. (1982) Hotspots, polar wander, Mesozoic convection and the geoid. *Nature*,
602 v. 297, pp. 391–393.

603 Arndt N., Bruzak, G. and Reischmann, T. (2001) The oldest continental and oceanic plateaus:
604 Geochemistry of basalts and komatiites of the Pilbara Craton, Australia. *Geol. Soc. Am.*,
605 Special Paper 352, pp. 359-387.

606 Artemieva, I.M., and Mooney, W.D. (2001) Thermal structure and evolution of Precambrian
607 lithosphere: A global study. *J. Geophys. Res.*, v. 106, pp. 16387–16414.

608 Aspler, L.B., and Chiarenzelli, J.R. (1998) Two Neoproterozoic supercontinents? Evidence from the
609 Paleoproterozoic. *Sedim. Geol.*, v. 120, pp. 75-104.

610 Ayer, J.A., Trowell, N.F., Madon, Z., Kamo, S., Kwok, Y.Y., Amelin, Y. (1999) Compilation of
611 the Abitibi greenstone belt in the Timmins-Kirkland lake area: revisions to stratigraphy and new
612 geochronological results. In: *Summary of Field Work and Other Activities 1999*. Ontario
613 Geological Survey, Open File Report 6000, pp. 1–14.

614 Barley, M.E., Eisenlohr, B.N., Groves, D.I., Perring, C.S., Vearncombe, J.R. (1989) Late
615 Archean convergent margin tectonics and gold mineralization: A new look at the Norseman
616 Wiluna Belt, Western Australia. *Geol.*, v. 17, pp. 826–829.

617 Barley, M.E., Krapez, B., Groves, D.I., Kerrich, R. (1998) The Late Archaean Bananzee:
618 metallogenic and environmental consequences of the interaction between mantle plumes,
619 lithospheric tectonics and global activity. *Precamb. Res.*, v. 91, pp. 65-90.

620 Baksi, A.K. (2003) Critical evaluation of $^{40}\text{Ar}/^{39}\text{Ar}$ ages for the Central Atlantic Magmatic
621 Province: timing, duration and possible migration of magmatic centers. In : Hames, W.E.,
622 McHome, J.G., Renne, P.R., and Ruppel, C. (Eds.), *The Central Atlantic Magmatic Province:
623 Insights From Fragments of Pangea*, American Geophysical Union Geophysical Monograph
624 136, pp. 77– 90.

625 Bateman, R., Costa, S., Swe, T., Lambert, D. (2001) Archaean mafic magmatism in the
626 Kalgoorlie area of the Yilgarn Craton, Western Australia: a geochemical and Nd isotopic study
627 of the petrogenetic and tectonic evolution of a greenstone belt. *Precamb. Res.*, v. 108, pp. 75–
628 112.

629 Bertrand, H., (1991) The Mesozoic Tholeiitic Province of Northwest Africa: A Volcano-
630 Tectonic Record of the Early Opening of Central Atlantic. In: Kampunzu, A.B., Lubala, R.T.
631 (Eds.), *Magmatism in Extensional Structural Settings. The Phanerozoic African Plate*. Berlin,
632 Heidelberg, New York: Springer-Verlag, pp. 147-188.

- 633 Bertrand H., Dostal J. and Dupuy C. (1982) Geochemistry of early mesozoic tholeiites from
1 634 Morocco. *Earth Planet. Sci. Lett.*, v. 58 , pp. 225-239.
- 2
3 635 Bertrand, H., Fornari, M., Marzoli, A., Sempere, T. and Feraud, G. (2005) Early Mesozoic rift-
4 636 related magmatism in the Bolivian Andes and Subandes : The southernmost record of the
5 637 Central Atlantic Magmatic Province. 6th International Symposium on Andean Geodynamics
6 638 (ISAG 2005, Barcelona), Extended Abstracts, pp. 111-114.
- 7
8 639 Beutel, E.K., Nomade, S., Fronabarger, A.K. and Renne, P.R. (2005) Pangea's complex breakup:
9 640 A new rapidly changing stress field model. *Earth Planet. Sci. Lett.*, v. 236, pp. 471-485.
- 10
11 641 Bleeker, W., Ketchum, J. W. F. & Davis, W. J. (1999a) The Central Slave Basement Complex,
12 642 Part II: Age and tectonic significance of high-strain zones along the basement-cover contact.
13 643 *Can. J. Earth Sci.*, v. 36, pp. 1111-1130.
- 14
15 644 Bleeker, W., Ketchum, J. W. F., Jackson, V. A. & Villeneuve, M. E. (1999b) The Central Slave
16 645 Basement Complex, Part I: Its structural topology and autochthonous cover. *CaEarth Sciences*,
17 646 36, 1083-1109. *History of the Earth*. Wiley, New York, pp. 113-129.
- 18
19 647 Bleeker, W. (2002) Archaean tectonics: a review, with illustrations from the Slave craton In:
20 648 Fowler, C. M. R., Ebinger, C. J. & Hawkesworth, C. J. (eds) *The Early Earth: Physical,*
21 649 *Chemical and Biological Development*. Geological Society, London, Special Publications, 199,
22 650 pp. 151-181.
- 23
24 651 Bruguier, O., Bosch, D., Pidgeon, R.T., Byrne, D.I., and Harris, L.B. (1999) U-Pb
25 652 geochronology of the Northampton Complex, Western Australia—Evidence for Grenvillian
26 653 sedimentation, metamorphism and deformation and geodynamic implications. *Contrib. Min.*
27 654 *Petrol.*, v. 136, pp. 258–272.
- 28
29 655 Bunge, H.-P., Baumgardner, J.R. (1995) Mantle convection modeling on parallel virtual
30 656 machines: *Computers in Physics*. v. 9, pp. 207–215.
- 31
32 657 Burke, K., Dewey, J.F. (1972) Plume generated triple junctions. Key indicators in applying plate
33 658 tectonics to old rocks. *J. Geol.*, v. 81, pp. 403-433.
- 34
35 659 Campbell, I.H., Griffiths, R.W. (1990) Implications of mantle plume structure for the evolution
36 660 of flood basalts. *Earth Planet. Sci. Lett.*, v. 99, pp. 79-93.
- 37
38 661 Cannon, W.F. (1992) The North American Midcontinent Rift beneath the Lake Superior region
39 662 with emphasis on its geodynamic evolution. *Tectonophys.*, v. 213, pp. 41–48.
- 40
41 663 Card, K.D. (1990) A review of the Superior Province of the Canadian Shield, a product of
42 664 Archean accretion. *Precambrian Res.*, v. 48, pp. 99–156.
- 43
44 665 Cawood, P.A., Buchan, C. (2007) Linking accretionary orogenesis with supercontinent
45 666 assembly. *Earth Sci. Rev.*, v. 82, pp. 217-256.
- 46
47 667 Cebria, J.M., Lopez-Ruiz, J., Doblas, M., Martins, L.T., Munha, J. (2003) Geochemistry of the
48 668 early Jurassic Messejana-Plasencia dyke (Portugal–Spain); implications on the origin of the
49 669 Central Atlantic Magmatic Province. *J. Petrol.*, v. 44, pp. 547–568.
- 50
51 670
52 671 Christensen, U.R. (1984) Heat transport by variable viscosity convection and implications for
53 672 the earth's thermal evolution. *Phys. Earth Planet. Int.*, v. 35, pp. 264-282.
- 54
55 673 Cobb, M.M., Cawood, P.A., Kinny, P.D., Fitzsimons, I.C.W. (2001) SHRIMP U-Pb zircon ages
56 674 for the Mullingarra Complex, Western Australia: Isotopic evidence for allochthonous blocks in
57
58
59
60
61
62
63
64
65

675 the Pinjarra orogen and implications for East Gondwana assembly. *Geol. Soc. Australia*
676 *Abstracts*, v. 64, pp. 21–22.

677 Coltice, N., Phillips, B.R., Bertrand, H., Ricard, Y., Rey, P. (2007) Global warming of the
678 mantle at the origin of flood basalts over supercontinents. *Geology*, v. 35, pp. 391-394.

679 Condie, K.C. (1998) Episodic continental growth and supercontinents: a mantle avalanche
680 connection? *Earth Planet. Sci. Lett.*, v. 163, pp. 97–108.

681 Condie, K.C. (2004) Supercontinents and superplume events: distinguishing signals in the
682 geologic record. *Phys. Earth Planet. Int.*, v. 146, pp. 319–332.

683 Courtillot, V., Jaupart, C., Manighetti, I., Tapponnier, P. and Besse, J. (1999) On causal links
684 between flood basalts and continental breakup. *Earth Planet. Sci. Lett.*, v. 166, pp. 177-195.

685 Cox, K.G. (1992) Karoo igneous activity, and the early stages of the break-up of Gondwanaland.
686 In: Storey, B.C., Alabaster, T., Pankhurst, R.J. (Eds.), *Magmatism and the Causes of Continental*
687 *Break-up*. *Geol. Soc. London, Special Publication 68*, pp. 137-148.

688 Corfu, F. (1987) Inverse age stratification in the Archaean crust of the Superior Province:
689 evidence for infra and subcrustal accretion from high resolution U–Pb zircon and monazite
690 ages. *Precambrian Res.*, v. 36, pp. 259–275.

691 Dalziel, I.W.D., Mosher, S., Gahagan, L.M. (2000) Laurentia-Kalahari collision and the
692 assembly of Rodinia. *J. Geol.*, v. 108, pp. 499-513.

693 Deckart, K., Féraud, G. and Bertrand, H. (1997) Age of Jurassic continental tholeiites of French
694 Guyana, Surinam and Guinea. Implications for the initial opening of the Central Atlantic Ocean.
695 *Earth Planet. Sci. Lett.*, v. 150, pp. 205-220.

696 Deckart, K., Bertrand, H. and Liegeois, J.P. (2005) Geochemistry and Sr, Nd, Pb isotopic
697 composition of the Central Atlantic Magmatic Province (CAMP) in Guyana and Guinea. *Lithos*,
698 v. 81, pp. 289-314.

699 DeMin, A., Piccirillo, E.M., Marzoli, A., Bellieni, G., Renne, P.R., Ernesto, M. and Marques, L.
700 (2003) The Central Atlantic Magmatic Province (CAMP) in Brazil: petrology, geochemistry,
701 $^{40}\text{Ar}/^{39}\text{Ar}$ ages, paleomagnetism and geodynamic implications. In : Hames, W.E., McHome,
702 J.G., Renne, P.R., and Ruppel, C. (Eds.), *The Central Atlantic Magmatic Province: Insights*
703 *From Fragments of Pangea*, American Geophysical Union Geophysical Monograph 136, pp.
704 209– 226.

705 Dirks, P. H. G. M., Jelsma, H. A. (1998) Horizontal accretion and stabilization of the Archaean
706 Zimbabwe Craton. *Geology*, v. 26, pp. 11-14.

707 Dosso, L. (1975) La méthode potassium-argon: datation de quelques dolerites de Mauritanie.
708 *Diplôme d'Ingénieur géophysicien, Université de Strasbourg*, 41p.

709 Duncan, A.R., Erlank, A.J., Marsh, J.S. (1984) Regional geochemistry of the Karoo igneous
710 province. In: A.J. Erlank (Eds), *Petrogenesis of the volcanic rocks of the Karoo province*. *Geol.*
711 *Soc. Special Publication of South Africa*, v. 13, pp. 355-388.

712 Duncan, R.A., Hooper, P.R., Rehacek, J., Marsh, J.S., Duncan, A.R. (1997) The timing and
713 duration of the Karoo igneous event, southern Gondwana. *J. Geophys. Res.*, v. 102, pp. 18127-
714 18138.

715 Dupuy, C., Marsh, J., Dostal, J., Michard, A., Testa, S. (1988) Asthenospheric and lithospheric
716 sources for Mesozoic dolerites from Liberia (Africa): trace element and isotopic evidence. *Earth*

717 Planet. Sci. Lett., v. 87, pp. 100-110.

718 Elburg, M., Goldberg, A. (2000) Age and geochemistry of Karoo dolerite dykes from northeast
719 Botswana. *J. Afr. Earth Sci.*, v. 31, pp. 539-554.

720 Ellam, R.M., Cox, K.G. (1989) A Proterozoic lithospheric source for Karoo magmatism:
721 evidence from the Nuanetsi picrites. *Earth Planet. Sci. Lett.*, v. 92, pp. 207-218.

722 Ellam, R.M., Cox, K.G. (1991) An interpretation of Karoo picrite basalts in terms of interaction
723 between asthenospheric magmas and the mantle lithosphere. *Earth Planet. Sci. Lett.*, v. 105, pp.
724 330-342.

725 Ellam, R.M., Carlson, R.W., Shirley, S.B. (1992) Evidence from Re-Os isotopes for plume-
726 lithosphere mixing in Karoo flood basalt genesis. *Nature*, v. 359, pp. 718-721

727 Ernst, R.E., Buchan, K.L. (2001) Large mafic magmatic events through time and links to
728 mantle-plume heads, in Ernst, R.E., and Buchan, K.L., eds., *Mantle plumes: Their*
729 *identification through time*. *Geol. Soc. Am. Special Paper 352*, pp. 483-575.

730 Ernst, R.E., Buchan, K.L. (2002) Maximum size and distribution in time and space of mantle
731 plumes: evidence from large igneous provinces. *J. Geodyn.*, v. 31, pp. 309-342.

732 Ernst, R.E., Buchan, K.L., Palmer, H.C. (1995) Giant dyke swarms: characteristics, distribution
733 and geotectonic applications. In: Baer, G., Heimann, A. (Eds.), *Physics and Chemistry of*
734 *Dykes*. Balkema, pp. 3-21.

735 Ernst, R.E., Wingate, M.T.D., Buchan, K.L., Li, Z.X. (2008) Global record of 1600-700Ma
736 Large Igneous Provinces (LIPs): Implications for the reconstruction of the proposed Nuna
737 (Columbia) and Rodinia supercontinents. *Precambrian Res.*, v. 160, pp. 159-178.

738 Farnetani, C. G.; Samuel, H. (2005) Beyond the thermal plume paradigm. *Geophys. Res. Lett.*,
739 v. 32, pp. L07311.

740 Glikson, A.Y., Stewart, A.J., Ballhaus, C.G., Clarke, G.L., Feeken, E.H.J., Leven, J.H.,
741 Sheraton, J.W., Sun, S.-S. (1996) Geology of the western Musgrave block, central Australia,
742 with particular reference to the mafic-ultramafic Giles Complex. *Australian Geol. Surv.*
743 *Organization Bull.*, v. 239, 206 p.

744 Grigne, C., Labrosse, S., Tackley, P.J. (2005) Convective heat transfer as a function of
745 wavelength. Implications for the cooling of the Earth. *J. Geophys. Res.*, v. 110, pp. B03409.

746 Guillou, L., Jaupart, C. (1995) On the effect of continents on mantle convection. *J. Geophys.*
747 *Res.*, v. 100, pp. 24217-2423.

748 Gurnis, M. (1988) Large-scale mantle convection and the aggregation and dispersal of
749 supercontinents. *Nature*, v. 332, pp. 695-699.

750 Hames, W.E., Renne, P.R., Ruppel, C. (2000) New evidence for geologically-instantaneous
751 emplacement of earliest Jurassic Central Atlantic magmatic province basalts on the North
752 American margin. *Geology*, v. 28, pp. 859-862.

753 Hanson, R.E., Martin, M.W., Bowring, S.A., Munyanyiwa, H. (1998) U-Pb zircon age for the
754 Umkondo dolerites, eastern Zimbabwe: 1.1 Ga large igneous province in southern Africa-East
755 Antarctica and possible Rodinia correlations. *Geology*, v. 26, pp. 1143-1146.

756 Hanson, R.E., Crowley, J.L., Bowring, S. A., Ramezani, J., Gose, W.A., Dalziel, I.W. D.,
757 Pancake, J. A., Seidel, E. K., Blenkinsop, T. G., Mukwakwami, J. (2004) Coeval large-scale

- 758 magmatism in the Kalahari and Laurentian cratons during Rodinia assembly. *Science*, v. 304,
1 759 pp. 1126-1129.
- 2
3 760 Hanson, R.E., Harmer, R.E., Blenkinsop, T.G., Buller, D.S., Dalziel, I.W.D., Gose, W.A., Hall,
4 761 R.P., Kampunzu, A.B., Key, R.M., Mukwakwami, J., Munyanyiwa, H., Pancake, J.A., Seidel,
5 762 E.K., Ward, E.K. (2006) Mesoproterozoic intraplate magmatism in the Kalahari Craton: A
6 763 review. *J. Afr. Earth Sci.*, v. 46, pp. 141-167.
- 7
8 764 Harrison, T. M.; Blichert-Toft, J.; Müller, W.; Albarede, F.; Holden, P.; Mojzsis, S. J. (2005)
9 765 Heterogeneous Hadean Hafnium: Evidence of Continental Crust at 4.4 to 4.5 Ga. *Science*, v.
10 766 310, pp. 1947-1950.
- 11
12 767 Hawkesworth, C.J., Marsh, J.S., Duncan, A.R., Erlank, A.J. and Norry, M.J. (1984) The role of
13 768 continental lithosphere in the generation of the Karoo volcanic rocks: evidence from combined
14 769 Nd- and Sr-isotope studies. In: Erlank, A.J. (Eds), *Petrogenesis of the volcanic rocks of the*
15 770 *Karoo province*. Geol. Soc. Special Publication South Africa 13, pp. 341-354.
- 16
17 771 Hawkesworth, C., Kelley, S., Turner, S., Le Roex, A., Storey, B. (1999) Mantle processes during
18 772 Gondwana break-up and dispersal. *J. Afr. Earth Sci.*, v. 28, pp. 239-261.
- 19
20 773 Heaman, L.M., Grotzinger, J.P. (1992) 1.08 Ga diabase sills in the Pahrum Group, California:
21 774 Implications for development of the Cordilleran miogeocline. *Geology*, v. 20, pp. 637-640.
- 22
23 775 Heather, K.B., Shore, G.T., van Breeman, O. (1995) The convoluted layer-cake: an old recipe
24 776 with new ingredients for the Swayze greenstone belt, southern Superior Province, Ontario. *Curr.*
25 777 *Res. 1995-C, Geol. Surv. Can.* 1-1
- 26
27 778 Heather, K.B. (1998) New insights on the stratigraphy and structural geology of the
28 779 southwestern Abitibi greenstone belt: implications for the tectonic evolution and setting of
29 780 mineral deposits in the Superior Province. In: *The First Age of Giant Ore Formation:*
30 781 *Stratigraphy, Tectonics and Mineralization in the Late Archean and Early Proterozoic.*
31 782 *Prospectors and Developers Association of Canada Annual Convention, Toronto*, pp. 63-101.
- 32
33 783 Hill, R.I. (1991) Starting plumes and continental break-up. *Earth Planet. Sci. Lett.*, v. 104, pp.
34 784 398-416.
- 35
36 785 Horstwood, M. S. A., Nesbitt, R. W., Noble, S. R., Wilson, J. F. (1999) U-Pb zircon evidence for
37 786 an extensive early Archean craton in Zimbabwe: a reassessment of the timing of craton
38 787 formatiostabilization, and growth. *Geology*, v. 27, pp. 707-710
- 39
40 788 Hernlund, J.W., Labrosse, S. (2007) Geophysically Consistent Values of the Perovskite to Post-
41 789 Perovskite Transition Clapeyron Slope, *Geophys. Res. Lett.*, v. 34, pp. L05309
- 42
43 790 Janney, P.E., Castillo, P.R. (2001) Geochemistry of the oldest Atlantic oceanic crust suggests
44 791 mantle plume involvement in the early history of the central Atlantic Ocean. *Earth Planet. Sci.*
45 792 *Lett.*, v. 192, pp. 291- 302.
- 46
47 793 Jaupart, C., Labrosse, S., Mareschal, J.-C. (2007) Temperatures, Heat and Energy in the Mantle
48 794 of the Earth, *Treatise on Geophysics*, v. 7, *Mantle dynamics* (Bercovici, Schubert, eds), pp. 253-
49 795 303.
- 50
51 796 Jelsma, H. A., Dirks, P. H. G. M. (2002) Neoproterozoic tectonic evolution in the Zimbabwe
52 797 Craton. In: Fowler, C. M. R., Ebinger, C. J. & Hawkesworth, C. J. (ed.) *The Early Earth:*
53 798 *Physical, Chemical and Biological Development*. Geological Society, London, Special
54 799 *Publications*, 199, pp. 183-211.
- 55
56
57
58
59
60
61
62
63
64
65

- 800 Jones, D.L., Duncan, R.A., Briden, J.C, Randall, D.E, MacNiocaill, C. (2001) Age of the
1 801 Batoka basalts, northern Zimbabwe, and the duration of Karoo Large Igneous Province
2 802 magmatism. *Geochem. Geophys. Geosys.*, v. 2, paper number 2000GC000110.
- 3
4 803 Jonhson, S.P., Oliver, G.J.H. (2000) Mesoproterozoic oceanic subduction, island arc formation
5 804 and the initiation of back-arc spreading in the Kibaran Belt of central, southern Africa: evidence
6 805 from the Ophiolite Terrane, Chewore Inliers, northern Zimbabwe. *Precambrian Res.*, v. 103, pp.
7 806 2000.
- 8
9
10 807 Jourdan F., Marzoli A., Bertrand H., Cosca M., Fontignie D. (2003) The northernmost CAMP:
11 808 $^{40}\text{Ar}/^{39}\text{Ar}$ age, petrology and Sr-Nd-Pb isotope geochemistry of the Kerforne dike, Brittany,
12 809 France, in: W.E. Hames, J.G. McHone, P.R. Renne, C. Ruppel (Eds), *The Central Atlantic
13 810 Magmatic Province, : insights from fragments of Pangea*. American Geophysical Union,
14 811 *Geophysical Monograph 136* , pp. 209-226.
- 15
16 812 Jourdan, F., Féraud, G., Bertrand, H., Kampunzu, A.B., Tshoso, G., Le Gall, B., Tiercelin,
17 813 J.J., Capiez P. (2004) The Karoo triple junction questioned: evidence from $^{40}\text{Ar}/^{39}\text{Ar}$ Jurassic
18 814 and Proterozoic ages and geochemistry of the Okavango dike swarm (Botswana). *Earth Planet.
19 815 Sci. Lett.*, v. 222, pp. 989-1006.
- 20
21 816 Jourdan, F., Féraud, G., Bertrand, H., Kampunzu, A.B., Tshoso, G., Watkeys, M.K., Le Gall., B.
22 817 (2005) The Karoo large igneous province: Brevity, origin, and relation with mass extinction
23 818 questioned by new $^{40}\text{Ar}/^{39}\text{Ar}$ age data. *Geology*, v. 33, pp. 745-748.
- 24
25 819 Jourdan, F., Féraud, G., Bertrand, H., Watkeys, M.K., Kampunzu, A.B., Le Gall B. (2006)
26 820 Basement control on dyke distribution in Large Igneous Provinces: case study of the Karoo
27 821 triple junction. *Earth Planet. Sci. Lett.*, v. 241, pp. 307-322.
- 28
29 822 Jourdan, F., Féraud, G., Bertrand, H., Watkeys, M.K. (2007a) From flood basalts to the onset of
30 823 oceanisation: example from the $^{40}\text{Ar}/^{39}\text{Ar}$ high-resolution picture of the Karoo large igneous
31 824 province. *Geochem. Geophys. Geosys.*, v. 8, pp. Q02002.
- 32
33 825 Jourdan, F., Féraud, G., Bertrand, H., Watkeys, M.K., Renne, P.R. (2007b) Distinct brief major
34 826 events in the Karoo large igneous province clarified by new $^{40}\text{Ar}/^{39}\text{Ar}$ ages on the Lesotho
35 827 basalts. *Lithos*, v. 98.
- 36
37 828 Jourdan, F., Bertrand, H., Schärer, U., Blichert-Toft, J., Féraud, G., Kampunzu, A.B. (2007c)
38 829 Major and trace element and Sr, Nd, Hf, and Pb isotope compositions of the Karoo large
39 830 igneous province, Botswana-Zimbabwe: Lithosphere versus mantle plume contribution. *J.
40 831 Petrol.*, v. 48, pp. 1043-1077.
- 41
42 832 Jourdan, F., Féraud, G., Bertrand, H., Watkeys, M.K., Renne, P.R. (2008) $^{40}\text{Ar}/^{39}\text{Ar}$ ages of the
43 833 sill complex of the Karoo large igneous province: implications for the Pliensbachian-Toarcian
44 834 climate change. *Geochem. Geophys. Geosys.*, in press
- 45
46 835 Jourdan, F., Féraud, G., Bertrand, H., Le Gall, B. (2008) Proterozoic to Jurassic LIP mantle
47 836 source evolution: example from the 180Ma-Karoo and 1.1Ga-Umkondo provinces, Africa.
48 837 *Geophys. Res. Abstract*, EGU General Assembly, Vienna.
- 49
50 838 Kemp, A. I. S., Hawkesworth, C. J. , Paterson, B. A., Kinny, P. D. (2006) Episodic growth of the
51 839 Gondwana supercontinent from hafnium and oxygen isotopes in zircon. *Nature*, v. 439, pp.
- 52
53 840 Knight, K.B., Nomade, S., Renne, P.R., Marzoli, A., Bertrand, H., Youbi, N. (2004) The Central
54 841 Atlantic Magmatic Province at the Triassic-Jurassic boundary : paleomagnetic and $^{40}\text{Ar}/^{39}\text{Ar}$
55 842 evidence from Morocco for brief, episodic volcanism. *Earth Planet. Sci. Lett.*, v. 228, pp. 143–
- 56
57
58
59
60
61
62
63
64
65

843 160.

844 Kusky, T. M. (1989) Accretion of the Archean Slave Province. *Geology*, v. 17, pp. 63-67.

845 Kusky, T. M. (1990) Evidence for Archean ocean opening and closing in the southern Slave
846 Province. *Tectonics*, v. 9, pp. 1533-1563.

847 Leitch, A.M., Davies, G.F., Wells, M. (1998) A plume head melting under a rifting margin.
848 *Earth Planet. Sci. Lett.*, v. 161, pp. 161-177.

849 Lenardic, A.; Moresi, L.-N.; Mühlhaus, H. (2003) Longevity and stability of cratonic
850 lithosphere: Insights from numerical simulations of coupled mantle convection and continental
851 tectonics. *J. Geophys. Res.*, v. 108, pp. B62303.

852 Li Z.X., Bogdanova, S.V., Collins, A.S., Davidson, A., De Waele, B., Ernst, R.E., Fitzsimons,
853 I.C.W., Fuck, R.A., Gladkochub, D.P., Jacobs, J., Karlstrom, K.E., Lu, S., Natapov, L.M., Pease,
854 V., Pisarevsky, S.A., Thrane, K., Vernikovsky, V. (2008) Assembly, configuration, and break-up
855 history of Rodinia: A synthesis. *Precambrian Res.*, v. 160, pp. 179-210.

856 Ludden, J., Hubert, C., Barnes, A., Milkereit, B., Sawyer, E. (1993) A three dimensional
857 perspective on the evolution of Archean crust: LITHOPROBE seismic reflection images in the
858 southwestern Superior Province. *Lithos*, v. 30, pp. 357-372.

859 Lowman, J.P., Jarvis, G.T. (1999) Thermal evolution of the mantle following continental
860 aggregation in 3D convection models. *Geophys. Res. Lett.*, v. 26, pp. 2649-2652.

861 Marsh, J.S., Hooper, P.R. Rehacek, J., Duncan, R.A., Duncan A.R. (1997) Stratigraphy and age
862 of Karoo basalts of Lesotho and implications for correlation within the Karoo igneous province.
863 In: Mahoney, J.J. and Coffin, M.F (Eds), *Large Igneous Province: Continental, Oceanic and*
864 *Planetary flood volcanism*, Geophysical Monograph series, Washinton D.C., pp. 247-272.

865 Marzoli, A., Renne, P.R., Piccirillo, E., Ernesto, E., Bellieni, G., De Min. A. (1999) Extensive
866 200-million-year-old continental flood basalts of the Central Atlantic Magmatic Province.
867 *Science*, v. 284, pp. 616-618.

868 Marzoli, A., Bertrand, H., Knight, K.B., Cirilli, S., Buratti, N., Vérati, C., Nomade, S., Renne,
869 P.R., Youbi, N., Martini, R., Allenbach, K., Neuwerth, R., Rapaille, C., Zaninetti, L., Bellieni,
870 G. (2004) Synchrony of the Central Atlantic magmatic province and the Triassic-Jurassic
871 boundary climatic and biotic crisis. *Geology*, v. 32, pp. 973-976.

872 May, P.R. (1971) Pattern of Triassic-Jurassic Diabase Dikes around the North Atlantic in the
873 Context of Predrift Positions of the Continents. *Geol. Soc. Am. Bull.*, v. 82, pp. 1285-1292.

874 McBride, J.H. (1991) Constraints on the structure and tectonic development of the early
875 Mesozoic south Georgia rift, southeastern United States; seismic reflection data processing and
876 interpretation. *Tectonics*, v. 10, pp. 1065-1083.

877 McHone, J.G. (2000) Non-plume magmatism and rifting during the opening of the Central
878 Atlantic Ocean. *Tectonophys.*, v. 316, pp. 287-296.

879 McHone, J.G., Anderson, D.L., Beutel, E.K., Fialko, Y.A. (2005) Giant dykes, flood basalts,
880 and plate tectonics: A contention of mantle models, in Foulger, G.R., Natland, J.H., Presnall,
881 D.C., and Anderson D.L., eds., *Plates, plumes and paradigms: Geological Society of America*
882 *Special Paper 388*, pp. 401-420.

883 Moorbath, S. (1978) Age and Isotope Evidence for the Evolution of Continental Crust. *Phil.*
884 *Trans. R. Soc. London A*, v. 288, pp. 401-412.

- 885 Morgan, W.J. (1981) Hotspot tracks and the opening of the Atlantic and Indian Ocean. In: C.
1 886 Emiliani (Eds), *The sea. volume 7: The Oceanic Lithosphere*. Wiley, New York.
- 2
3 887 Morgan, W.J. (1983) Hotspot tracks and the early rifting of the Atlantic. *Tectonophys.*, v. 94, pp.
4 888 123-139.
- 5
6 889 Munyanyiwa, H. (1999) Geochemical study of the Umkondo dolerites and lavas in Chimanimani
7 890 and Chipige Districts (eastern Zimbabwe) and their regional implications. *J. Afr. Earth Sci.*, v.
8 891 28, pp. 349-365.
- 9
10 892 Nicholson, S.W., Shirey, S.B. (1990) Midcontinent rift volcanism in the Lake Superior region:
11 893 Sr, Nd, and Pb isotopic evidence for a mantle plume origin. *J. Geophys. Res.*, v. 95, pp. 10851–
12 894 10868.
- 13
14 895 Nomade, S., Knight, K.B., Beutel, E., Renne, P.R., Vérati, C., Féraud, G., Marzoli, A., Youbi,
15 896 N., Bertrand, H. (2007) Chronology of the Central Atlantic Magmatic Province: Implications for
16 897 the Central Atlantic rifting processes and the Triassic–Jurassic biotic crisis. *Palaeogeog.*
17 898 *Palaeoclim. Palaeoecol.*, v. 244, pp. 326-344.
- 18
19
20 899 Oyarzun, R., Doblaz, M., Lopez-Ruiz, J., Cebria, J.M. (1997) Opening of the central Atlantic
21 900 and asymmetric mantle upwelling phenomena: Implications for long-lived magmatism in
22 901 western North Africa and Europe. *Geology*, v. 25, pp. 727-730.
- 23
24 902 Paces, J.B., Bell, K. (1989) Non-depleted sub-continental mantle beneath the Superior Province
25 903 of the Canadian Shield: Nd-Sr isotopic and trace element evidence from Midcontinent Rift
26 904 basalts. *Geochim. Cosmochim. Acta*, v. 53, pp.2023-2035
- 27
28
29 905 Pegram, W.J. (1990) Development of continental lithospheric mantle as reflected in the
30 906 chemistry of the Mesozoic Appalachian Tholeiites, U.S.A.. *Earth Planet. Sci. Lett.*, v. 97, pp.
31 907 316– 331.
- 32
33 908 Percival, J.A., Williams, H.R. (1989) The Late Archaean Quetico accretionary complex,
34 909 Superior Province, Canada. *Geology*, v. 17, pp. 23–25.
- 35
36 910 Phillips, B.R., Bunge, H.-P. (2005) Heterogeneity and time dependence in 3D spherical mantle
37 911 convection models with continental drift. *Earth Planet. Sci. Lett.*, v. 233, pp. 121–135.
- 38
39 912 B. R. Phillips, Bunge, H.-P. (2007). Supercontinent cycles disrupted by strong mantle plumes.
40 913 *Geology*, v. 35, pp. 847-850.
- 41
42 914 Puffer, J.H. (2001) Contrasting high field strength element contents of continental flood basalts
43 915 from plume versus reactivated-arc sources. *Geology* 29, 675–678. Rey, P.F., Philippot, P., and
44 916 Thebaud, N., 2003, Contribution of mantle plumes, crustal thickening and greenstone
45 917 blanketing to the 2.75–2.65 Ga global crisis. *Precambrian Res.*, v. 127, pp. 43–60.
- 46
47
48 918 Ricard, Y., Richards, M.A., Lithgow-Bertelloni, C., LeStunff, Y. (1993), A geodynamic model
49 919 of mantle density heterogeneity. *J. Geophys. Res.*, v. 98, pp. 21895–21909.
- 50
51 920 Richards, M.A., Duncan, R.A., Courtillot, V.E. (1989) Flood basalts and hot-spot tracks: plume
52 921 heads and tails. *Science*, v. 246, pp. 103-107.
- 53
54 922 Rino, S., Komiya, T., Windley, B. F., Katayama, I., Motoki, A., Hirata, T. (2004) Major episodic
55 923 increases of continental crustal growth determined from zircon ages of river sands; implications
56 924 for mantle overturns in the early Precambrian. *Phys. Earth Planet. Int.*, v. 146, pp. 369–394.
- 57
58 925 Sahabi, M., Aslanian, D., Olivet, J.L. (2004) A new starting point for the history of the central
59 926 Atlantic, *Compte Rendus Geoscience*, v. 336, pp. 1041-1052.
- 60
61
62
63
64
65

- 927 Schaltegger, U., Guex, J., Bartolini, A., Schoene, B. and Ovtcharova, M. (2008) Precise U-Pb age
1 928 constraints for end Triassic mass extinction, its correlation to volcanism and Hettangian post-
2 929 extinction recovery. *Earth Planet. Sci. Lett.*, v. 267, pp. 266-275.
- 930 Shastri, L.L., Chamberlain, K.R., Bowring, S.A. (1991) Inherited zircon from ca. 1.1 Ga mafic
5 931 dikes, NW Arizona. *Geol. Soc. Am. Abstracts with Programs* 23, pp.93.
- 932 Shirey, S.B., Klewin, K.W., Berg, J.H., Carlson, R.W. (1994) Temporal changes in the sources
8 933 of flood basalts: Isotopic and trace element evidence from the 1100 Ma old Keweenawan
9 934 Mamainse Point Formation, Ontario, Canada. *Geochim. Cosmochim. Acta*, v. 58, pp. 4475–
10 935 4490.
- 936 Sweeney, R.J., Watkeys, M.K. (1990) A possible link between Mesozoic lithospheric
13 937 architecture and Gondwana flood basalts. *J. Afr. Earth Sci.*, v. 10, pp. 707-716.
- 938 Sleep, N.H. (1990) Hot spots and mantle plumes: some phenomenology. *J. Geophys. Res.*, v. 95,
16 939 pp. 6715–6736.
- 940 Sweeney, R.J., Falloon, T.J., Green, D.H., Tatsumi, Y. (1991) The mantle origins of Karoo
19 941 picrites. *Earth Planet. Sci. Lett.*, v. 107, pp. 256-271.
- 942 Sweeney, R.J., Duncan, A.R., Erlank, A.J. (1994) Geochemistry and petrogenesis of Central
22 943 Lebombo basalts from the Karoo Igneous Province. *J. Petrol.*, v. 35, pp. 95-125.
- 944 Tackley, P.J. (2000) Mantle Convection and Plate Tectonics: Toward an Integrated Physical and
25 945 Chemical Theory. *Science*, v. 288, pp. 2002-2007.
- 946 Thurston, P.C. (2002) Autochthonous development of Superior Province greenstone belts?
28 947 *Precambrian Res.*, v. 115, pp. 11–36.
- 948 Verati, C., Bertrand, H. and Féraud, G. (2005) The farthest record of the Central Atlantic
31 949 Magmatic Province into West Africa craton: Precise $^{40}\text{Ar}/^{39}\text{Ar}$ dating and geochemistry of
32 950 Taoudenni basin intrusives (northern Mali). *Earth Planet. Sci. Lett.*, v. 235, pp. 391– 407.
- 951 Verati, C., Rapaille, C., Féraud, G., Marzoli, A., Bertrand, H., Youbi, N. (2007) $^{40}\text{Ar}/^{39}\text{Ar}$ ages
35 952 and duration of the Central Atlantic Magmatic Province volcanism in Morocco and Portugal and
36 953 its relation to the Triassic–Jurassic boundary. *Palaeogeo. Palaeoclim. Palaeoecol.*, v. 244, pp.
37 954 308-325.
- 955 Vervoort, J.D., Green, J.C. (1997) Origin of evolved magmas in the Midcontinent rift system,
41 956 northeast Minnesota: Nd-isotope evidence for melting of Archean crust. *Can. J. Earth Sci.*, v.
42 957 34, pp. 521–535.
- 958 Vervoort, J.D., Wirth, K., Kennedy, B., Sandland, T., Harpp, K.S. (2007) The magmatic
45 959 evolution of the Midcontinent rift: New geochronologic and geochemical evidence from felsic
46 960 magmatism. *Precambrian Res.*, v. 157, pp. 235-268.
- 961 Williams, H., Hoffman, P.F., Lewry, J.F., Monger, J.W.H., Rivers, T. (1991) Anatomy of North
50 962 America: thematic portrayals of the continent. *Tectonophys.*, v. 187, pp. 117-134.
- 963 Wingate, M.T.D., Pirajno, F., Moris, P.A. (2004) Warakurna large igneous province: A new
53 964 Mesoproterozoic large igneous province in west-central Australia. *Geology*, v. 32, pp. 105-108.
- 965 Wyman, D.A., Kerrich, R., Polat, A. (2002) Assembly of an Archean cratonic mantle
56 966 lithosphere and crust: plume–arc interaction in the Abitibi–Wawa subduction–accretion
57 967 complex. *Precambrian Res.*, v. 115, pp. 37 – 62.

968 van der Westhuizen, W.A., de Bruijn, H., Meintjes, P.G. (1991) The Ventersdorp Supergroup:
1 969 an overview. *J. Afr. Earth Sci.*, v. 13, pp. 83–105.
2
3 970 Watkeys, M.K. (2002) Development of the Lebombo rifted volcanic margin of southeast Africa.
4 971 In: M.A. Menzies, S.L. Klemperer, C.J. Ebinger, J. Baker (Eds), *Volcanic rifted margin*. *Geol.*
5 972 *Soc. Am. Special Paper*, Colorado, pp. 29-48.
6
7 973 Wigley, R. (1995) The geochemistry of the Karoo igneous volcanic and intrusive rocks of
8 974 Botswana, University of Cape Town, PhD thesis, 182 p.
9
10 975 Wilson, M. (1997) Thermal evolution of the Central Atlantic passive margins : Continental
11 976 break-up above a Mesozoic super-plume. *J. Geol. Soc. London*, v. 154, pp. 491-495.
12
13 977 Yale, L. B.; Carpenter, S. J. (1998) Large igneous provinces and giant dike swarms: proxies for
14 978 supercontinent cyclicality and mantle convection. *Earth Planet. Sci. Lett.*, v. 163, pp. 109-122.
15
16 979 Zhao, J.-X., McCulloch, M.T. (1993), Melting of a subduction-modified continental lithospheric
17 980 mantle: Evidence from Late Proterozoic mafic dike swarms of central Australia. *Geology*, v. 21,
18 981 pp. 463–466.
19
20 982 Zhong, S., Gurnis, M. (1993) Dynamic feedback between a continentlike raft and thermal
21 983 convection. *J. Geophys. Res.*, v. 98, pp. 12219–12232.
22
23 984
24
25
26
27
28
29
30
31
32
33
34
35
36
37
38
39
40
41
42
43
44
45
46
47
48
49
50
51
52
53
54
55
56
57
58
59
60
61
62
63
64
65

1 985 Fig.1: Snapshots of temperature for six spherical convection models. The temperature range
2 986 spans nondimensional values of 0.013 (blue) to 0.036 (red). Gray caps indicate the surface
3
4 987 location of fixed continents. The models contain A) two antipodal continents, each of which
5
6 988 covers 5% of the surface, B) one continent covering 10% of the surface, C) two continents with
7
8 989 10% coverage, D) one continent with 20% coverage, E) two continents with 15% coverage, and
9
10 990 F) one continent with 30% coverage. Respective pairs from left to right give a sense for the
11
12 991 impact on the mantle due to the aggregation of two smaller continents into a single large
13
14 992 continent. An apparent impact on subcontinental temperature occurs only once the size of an
15
16 993 individual continent reaches 20% coverage. The full supercontinent of F) is unique in promoting
17
18 994 a strong hemispheric scale hot anomaly shown by the far reaching extent of warm colors,
19
20 995 indicative of global mantle warming.

21
22 996
23
24 997 Fig.2: Subcontinental nondimensional temperature excess of the aggregated state relative to the
25
26 998 two continent dispersed state as a function of total continental coverage and Rayleigh number.
27
28 999 The $Ra = 10^7$ values correspond to the models shown in Fig. 1.

29
30
31 1000 Fig.3: Extension of the Central Atlantic Magmatic Province at 200Ma.

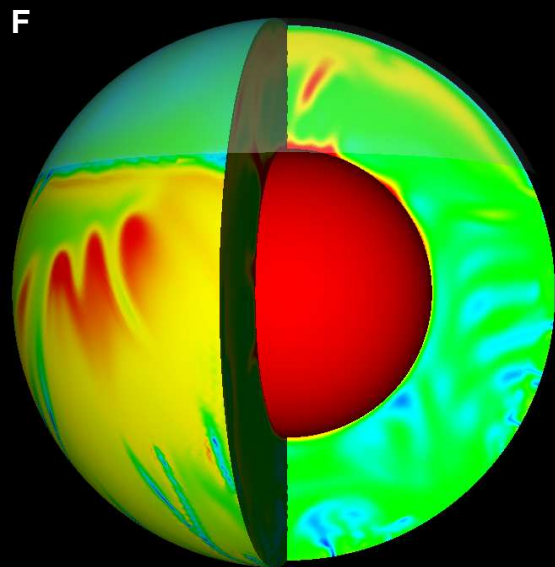
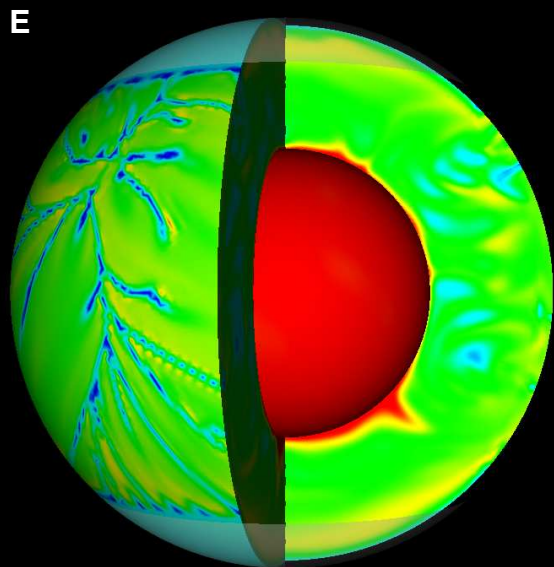
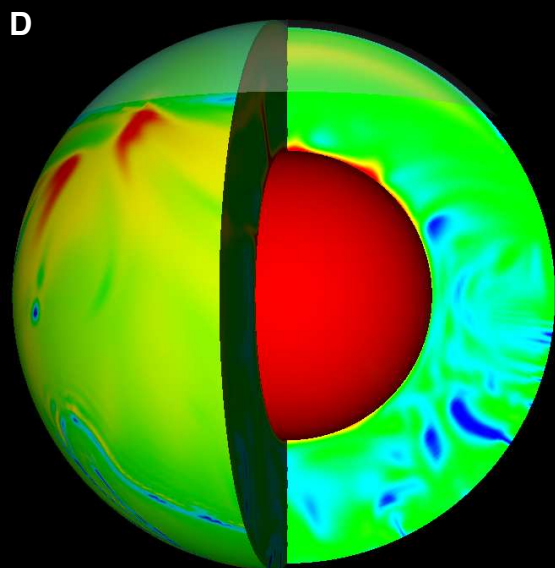
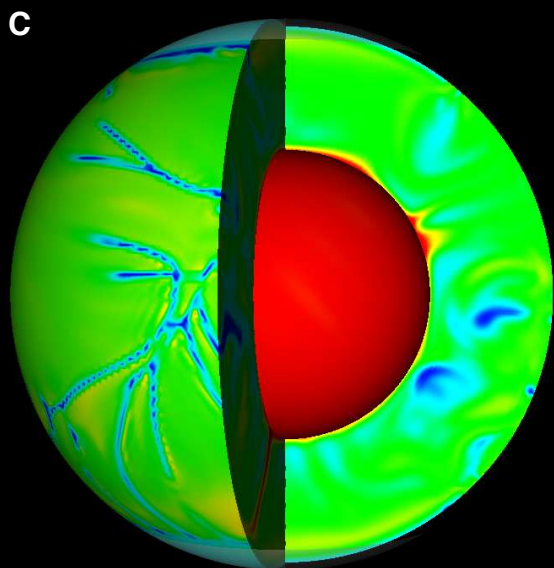
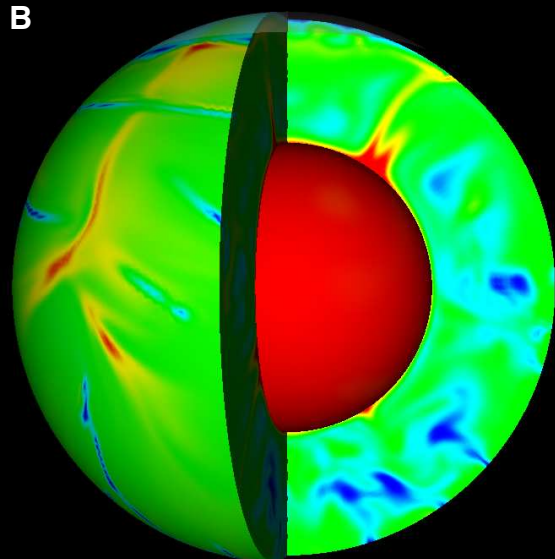
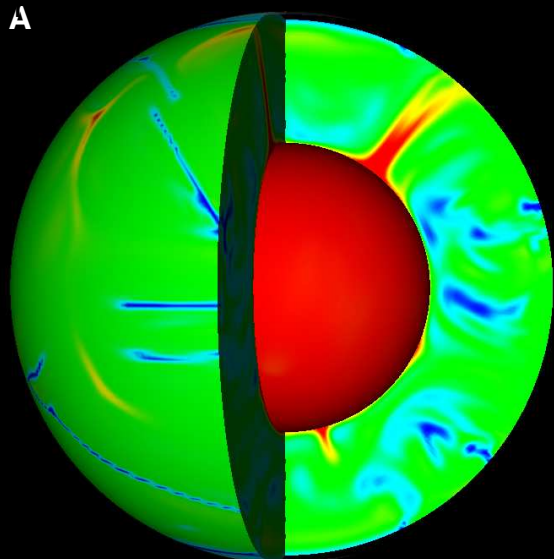
32
33 1001 Fig.4: Extension of the Karoo Province at 180Ma.

34
35 1002 Fig.5: Estimated extension of the Umkondo, Warakurna and Keweenawan provinces at the time
36
37 1003 of Rodinia aggregation.

38
39
40 1004 Fig.6: Continental warming following the emplacement of a 6 km thick CFB on a 2.75 Ga old
41
42 1005 continental crust (heat production of 10^{-6} W m^{-3} , mantle heat flow of 0.025 W m^{-2} , 1000 J mol^{-1} ,
43 1006 thermal diffusivity of $0.9 \cdot 10^{-6} \text{ m}^2 \text{ s}^{-1}$, continental crust thickness of 40 km). a/ Geotherm at to,
44
45 1007 to+5my, to+25 my, to+50 my, to+100 my, to+250 my and b/ evolution of the Moho temperature
46
47 1008 after emplacement of a 6 and 12 km thick CFB. Continental warming and anatexis is
48
49 1009 inescapable and does not require the direct heat input from a mantle plume.

50
51
52 1010

53
54
55
56
57
58
59
60
61
62
63
64
65

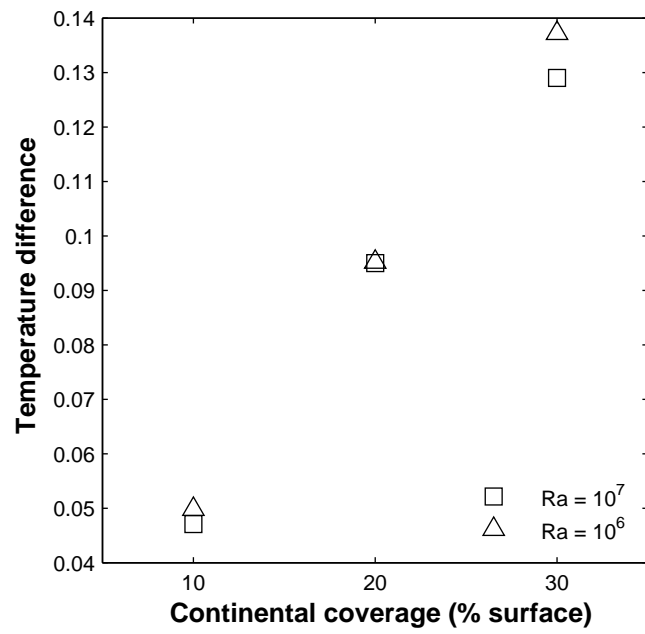


1.52

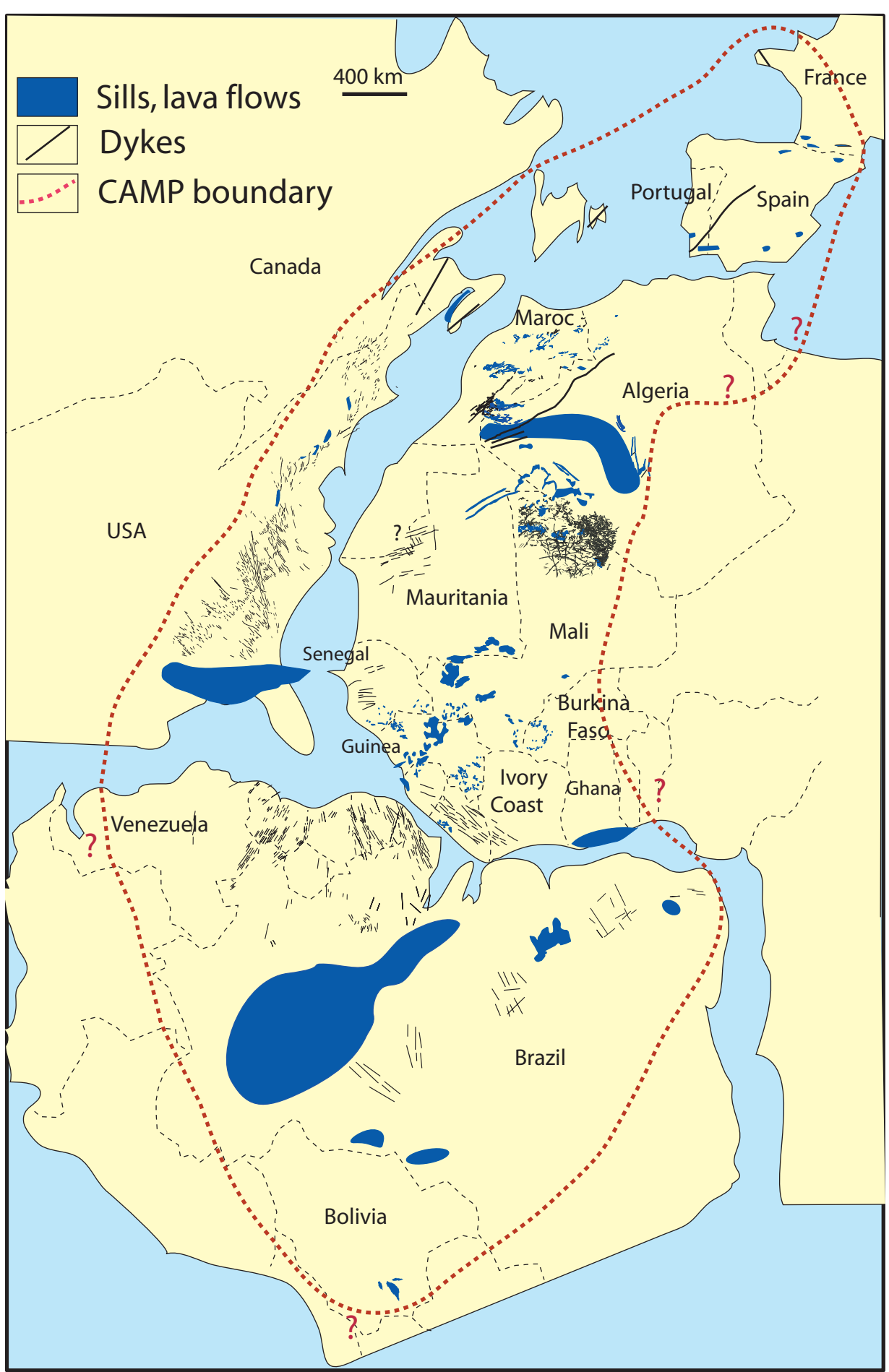
Temperature

0.55

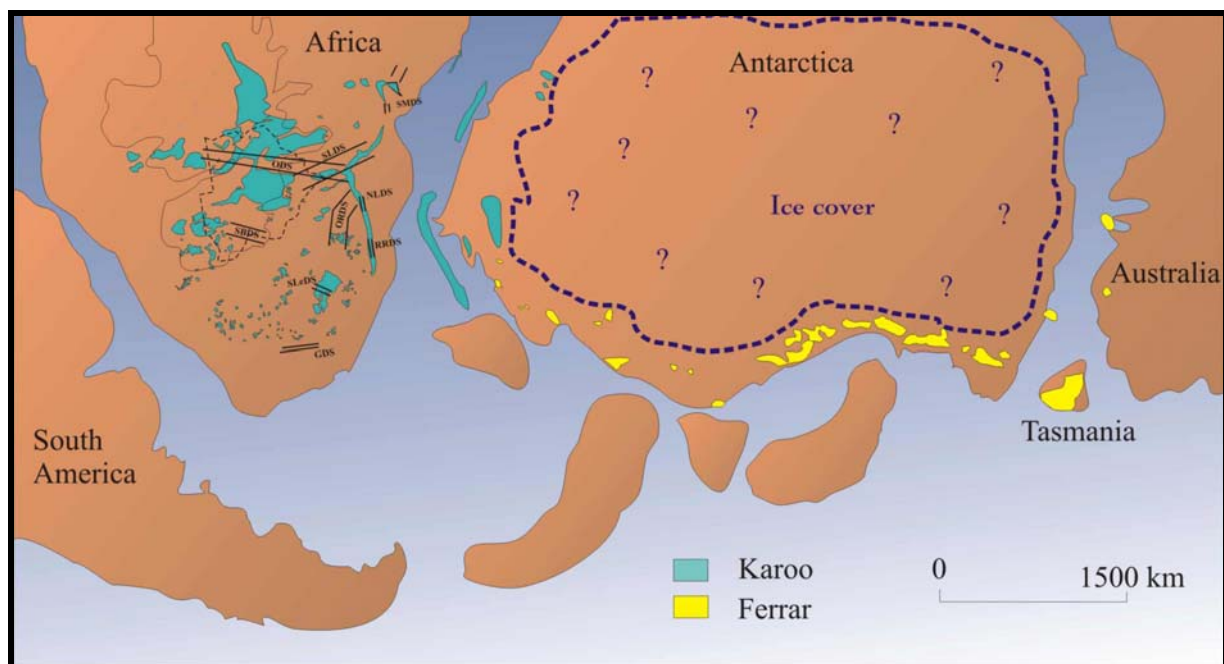
Figure



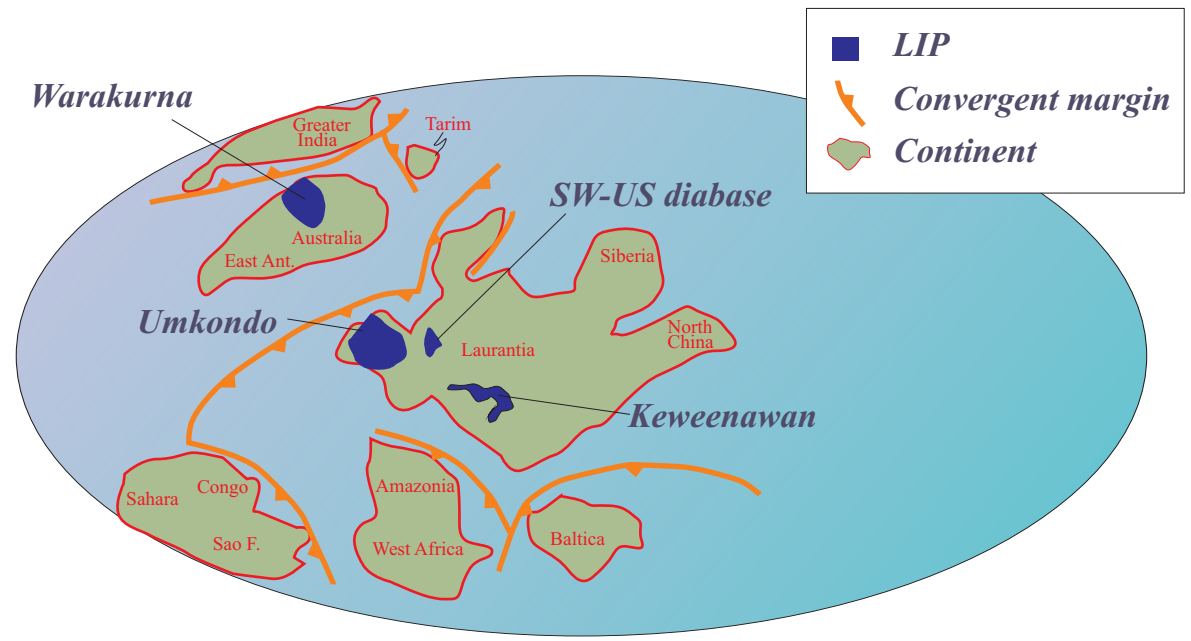
Figure



Figure



Figure



Figure

